

AMERICAN UNIVERSITY OF BEIRUT

OPTIMAL PLANNING OF A MICROGRID USING
ELECTRIC VEHICLES AND DISTRIBUTED ENERGY
RESOURCES UNDER GRID'S BLACKOUTS

by
ZEINA MAZEN ZWEINI

A thesis
submitted in partial fulfillment of the requirements
for the degree of Master of Engineering
to the Department of Electrical and Computer Engineering
of the Maroun Semaan Faculty of Engineering and Architecture
at the American University of Beirut

Beirut, Lebanon
July 2021

AMERICAN UNIVERSITY OF BEIRUT

OPTIMAL PLANNING OF A MICROGRID USING
ELECTRIC VEHICLES AND DISTRIBUTED ENERGY
RESOURCES UNDER GRID'S BLACKOUTS

by
ZEINA MAZEN ZWEINI

Approved by:

Dr. Riad Chedid, Professor
Department of Electrical and Computer Engineering



Advisor

Dr. Farid Chaaban, Professor
Department of Electrical and Computer Engineering



Member of Committee

Dr. Sami Karaki, Professor
Department of Electrical and Computer Engineering

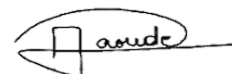
Sami
Karaki



Digitally signed by Sami Karaki
DN: c=cc, o=Sami Karaki, ou=AEU,
ou=ECE Department,
email=skaraki@aub.edu.lb,
c=LB
Date: 2021.08.23 16:17:01
+0300

Member of Committee

Dr. Dany Abou Jaoude, Assistant Professor
Department of Mechanical Engineering



Member of Committee

Date of thesis defense: July 1st, 2021

AMERICAN UNIVERSITY OF BEIRUT

THESIS RELEASE FORM

Student Name: Zweini Zeina Mazen

I authorize the American University of Beirut, to: (a) reproduce hard or electronic copies of my thesis; (b) include such copies in the archives and digital repositories of the University; and (c) make freely available such copies to third parties for research or educational purposes:

- As of the date of submission
- One year from the date of submission of my thesis.
- Two years from the date of submission of my thesis.
- Three years from the date of submission of my thesis.

Signature
Zeina Zweini

Date
September 9, 2021

ACKNOWLEDGEMENTS

I would like to express my deepest thanks and gratitude to my thesis advisor Prof. Riad Chedid for his continuous support, encouragement and guidance in every stage of my research project. His expertise was invaluable to maintain my progress on track and to bringing this research into light.

I am deeply grateful as well to Prof. Sami Karaki and Prof. Farid Chaaban for their supervision and professional guidance and support during this and other related projects.

I want to extend my sincere thanks to Prof. Dany Abou Jaoude for his insightful feedback that sharpened my thinking and brought my work to a higher level.

Lastly, I want to express my appreciation to all my colleagues and mentors in the department of electrical and computer engineering for their endless efforts and help throughout this journey.

ABSTRACT OF THE THESIS OF

Zeina Mazen Zweini

for

Master of Engineering

Major: Energy and Power Systems

Title: Optimal Planning of a Microgrid Using Electric Vehicles and Distributed Energy Resources Under Grid's Blackouts

Renewable energy sources have developed as a substitute to supply the increasing energy demand, replace finite energy resources such as fossil fuels, mitigate climate change, and play a major role in sustainable development. Lebanon has been experiencing for decades an intermittent and unreliable power supply. Thus, the overall purpose of this paper is to reshape the power supply system of the American University of Beirut (AUB) campus - currently characterized by consistent daily grid blackout hours - by shifting the electricity deficit to renewable distributed energy resources rather than the heavy reliance on on-site diesel generators. The concept of combining PV systems and battery storage systems (BSS) represents a promising solution to grid outages.

This study also considers the use of electric vehicles (EVs) as a substitute to conventional fuel-based vehicles used for work-related trips. Additionally, to help AUB community commute easily on campus, the feasibility of integrating an e-scooter sharing system has been investigated in this work. Due to the limited space available on campus to install large BSS and despite the preliminary function that both transportation systems play, they can aid in supplying load demand by acting as a virtual battery storage system in absence of a large transportation demand.

To achieve those targets, two main optimization stages were implemented. The first is a multi-objective optimization problem formulated to converge to an optimal PV and BSS capacity and to an optimal charge rate to be imposed on using e-scooter service (in \$/km). This has been fulfilled by optimizing a rule-based energy management system (EMS) with the aid of one of the following nonlinear optimization techniques: Particle Swarm Optimization (PSO) and FMINCON solver via YALMIP parser. Whereas the second optimization level operates the optimally configured MG under an optimal EMS which finds the optimal performance of such MG using convex optimization technique.

Results showed that the proposed system was able to minimize campus daily operational costs, contribute to a better adoption of clean energy resources, reduce diesel dependency during outages, and decrease power purchased at peak-tariff hours. Such findings suggest that the proposed system is a successful model that can help Lebanese community resolve the grid's blackout issues and reduce diesel dependency in meeting load demand.

TABLE OF CONTENTS

ACKNOWLEDGEMENTS	1
ABSTRACT	2
ILLUSTRATIONS	6
TABLES	8
ABBREVIATIONS	9
INTRODUCTION	12
LITERITURE REVIEW	15
2.1. Research Efforts on Determining the Optimal Configuration of a MG:	15
2.2. Research Efforts Related to EVs Adoption and Contribution in the Energy Sector:	16
2.3. Research Efforts Related to E-Scooters Service:.....	17
2.4. Research Efforts on MGs EMS and Its Associated Optimization Techniques: ..	21
PROBLEM FORMULATION	22
SYSTEM MODELLING	25
4.1. Photovoltaic Modelling:	25
4.2. EDL (Grid) Modelling:	29
4.3. Battery Storage System (BSS) Modelling:	30

4.4. Electric Demand Modelling:.....	32
4.5. Diesel Generator Modelling:	33
4.6. Electric vehicle (EV) Modelling:.....	34
4.7. E-Scooters Modelling:	37
4.8. Electric Vehicle Transportation Demand Modelling.....	40
4.9. E-Scooter Transportation Demand Modelling:.....	41
METHODOLOGY	48
5.1. First Optimization Level:.....	49
5.1.1 Proposed Rule-Based Energy Management System:.....	51
5.1.2. Proposed Optimization Techniques:	55
5.2. Second Optimization Level:	59
5.2.1. Proposed Optimization Technique:	60
RESULTS	65
6.1. First Level optimization.....	66
6.2. Second Optimization Results.....	67
6.3. Financial and Sensitivity Analysis.....	71
6.3.1 Current Operating System Financial Analysis:	71
6.3.2 Proposed System Financial Analysis	71
6.3.3. Sensitivity Analysis	74
Conclusion	77
APPENDIX	78

REFERENCES81

ILLUSTRATIONS

Figure	Page
1. Annual ambient temperature profile of AUB campus during the year of 2017.	27
2. Annual solar irradiance profile of AUB campus during the year of 2017.....	27
3. Annual PV output power per module.	28
4. AUB annual load demand profile as in 2017.....	33
5. Location of the e-scooters charging/docking stations.....	38
6. Frequency of the work-related trips covered by the service vehicles expressed in days per week.....	41
7. Typical weekday hourly e-scooter transportation demand.	43
8. Hourly e-scooter transportation demand for a typical weekday/weekend expressed in kilometers.....	44
9. E-scooter’s yearly transportation demand expressed in kilowatt-hour considering seasonal, daily and hourly variations for the sample population considered.....	45
10. Users satisfaction index as a function of the charge cost per kilometer.	47
11. Rule-Based EMS.....	54
12. Particle swarm optimization flow chart [85].	56
13. FMINCON solver multi-initialization grid in terms of PV capacity, BSS capacity, and \$/km. Blue stars represent distinct structured initializations while the red ones represent random initialization in the search space. In total, the simulation was performed for 1150 initial points.	58
14. Particle Swarm Optimization multi-initialization grid as a function of PV capacity, BSS capacity, and \$/km. Blue stars represent distinct structured initializations while red one represent random initialization in the search space. In total, simulations was performed considering 170 initial point.	58
15. Impact of loan's interest rates increase on the system's yearly savings	75
16. Impact of different donation percentages on the system’s yearly savings.	76
17. Respondents perspective on integrating an e-scooter commuting service on campus.	78
18. Respondent's perceptions on various e-scooter service attributes in terms of safety measures (scooter lanes and speed limit), network coverage (stations locations), accessibility (subscriptions and pay per use) and time window and convenience.	79

19. Ratings of different price ranges..... 80

TABLES

1. Table 1:PV module characteristics	28
2. Table 2: Scheduled daily grid's outage.....	30
3. Table 3: Grid's triple tariff rate scheme	30
4. Table 4: Battery's annual retention regime.....	31
5. Table 5: Annual energy demand of AUB	33
6. Table 6: AUB installed diesel generators set.....	34
7. Table 7: AUB service vehicles data.....	35
8. Table 8: Proposed AUB electric service vehicles.....	35
9. Table 9: E-scooter safety and electrical characteristics	37
10. Table 10: E-Scooters charging/docking stations specifications	38
11. Table 11: Typical weekly EVs transportation energy demand profile (kWh)....	41
12. Table 12: AUB population data	42
13. Table 13: Weights assigned to the MGs energy sources.	60
14. Table 14: Technical and economic input specifications of the MG components.	66
15. Table 15: First stage optimization results.	67
16. Table 16: Annual performance of the proposed system in comparison to the existing one.	68
20. Table 17:The proposed system carbon footprint in comparison to the existing one.....	69
21. Table 18: Performance evaluation of the current operating system over a 12 year period.	71
22. Table 19: Yearly financial and energy outcomes of the proposed system.	73

ABBREVIATIONS

AUB: American University of Beirut
DERs: Distributed Energy Resources
PV: Photovoltaic System
BSS: Battery Storage System
EVs: Electric Vehicles
DG: Distributed Generation
MGs: Microgrids
EMS: Energy Management System
V2M: Vehicle to Microgrid
V2V: Vehicle to Vehicle
V2H: Vehicle to home
LEVs: Light Electric Vehicles
PSO: Particle Swarm Optimization
EDL: Electricité du Liban
V2M: Vehicle to microgrid
M2V: Microgrid to vehicle
STC: Standard test conditions
 $I_{SC}(t)$: Short circuit current at time t under operating conditions
 $V_{OC}(t)$: Open-circuit voltage at time t under operating conditions
 s : Solar irradiance in kW/m^2 at any time t
 $FF(t)$: Actual fill factor of the module
 $FF_0(t)$: Ideal fill factor of the module.
 $V_{OC,0}(t)$: Normalized open-circuit voltage at any time t
 q : Charge of an electron
 n : Ideality factor assumed equal to 1
 k : Boltzmann's constant
 $T_C(t)$: Module's temperature at any time t in $^{\circ}\text{C}$
 R_s : Module series resistance
 $r_s(t)$: Normalized module series resistance at any time t
 $T_a(t)$: Module ambient temperature
NOCT: Nominal operating cell temperature provided by the manufacturer.
 η^{PV} : Efficiency of the PV inverter
 $r_{s,STC}$: Normalized series resistance under STC
 FF_{STC} : Actual fill factor under STC
 $FF_{O,STC}$: Ideal fill factor under STC
 $V_{OC,0,STC}$: Normalized open circuit voltage under STC
 $P^{PV,r}$: PV system's rated capacity in kW
 CC^{PV} : PV system capital cost in \$
 OM^{PV} : PV system operation and maintenance cost in \$/year
 AP^{PV} : PV system annual payment in \$
 $CRF^{PV}(i, N)$: PV system loan's capital recovery factor at an interest i and for N years
 COE^{PV} : PV system's cost of energy in \$/kWh
 $P^{EDL}(t)$: Power supplied in kW by the grid at time slot t
 $EDL_{profile}(t)$: Binary decision variable representing the grid state (ON/OFF) at time t .

$P_{DC}^{BSS}(t)$: BSS DC charging/discharging rate in kW
 $P_{dch}^{BSS}(t)$: BSS AC discharging power in kW
 $P_{ch}^{BSS}(t)$: BSS AC charging power in kW at time t
 η^{BSS} : BSS inverters efficiency
 $E^{BSS}(t)$: BSS energy in kWh at time t
 $SOC(t)$: BSS state of charge of the battery at each time t
 C^{BSS} : BSS nominal capacity in Ah
 V : BSS nominal voltage
 a : BSS self-discharging factor
 SOH : BSS's state of health.
 AP^{BSS} : BSS annual loan payment in \$
 CC^{BSS} : BSS capital cost in \$
 OM^{BSS} : BSS operation and maintenance cost in \$/year
 COE^{BSS} : BSS cost of energy in \$/kWh
 $EDL_{Tariff}(t)$: Grid electricity tariff at time t in \$/kWh
 $FC(t)$: Diesel generator's fuel consumption in L at time t
 $P^{Die}(t)$: Diesel generator's actual output power in kW
 $P^{Die,r}$: Diesel Generator's rated power in Kw
 γ and β : Diesel generator's fuel consumption coefficients
 $CF(t)$: Diesel fuel cost of the diesel generator in \$ at time t
 ψ : Diesel cost in \$/L at time t
 CC^{EV} : Total capital cost of the EV fleet in \$
 $CC(i)$: Capital cost of $EV(i)$ in \$
 CRF^{EV} : EVs capital recovery factor for N years at interest rate i ,
 $\sum_{t=1}^{8760} P_L^{EV}(t)$: EVs annual discharged energy to supply load demand in kW
 $\sum_{t=1}^{8760} P_{trans}^{EV}(t)$: EVs annual discharged energy to supply transportation demand in kW
 N^{sc} : Number of e-scooters
 $N^{Station}$: Number of charging/docking stations
 CRF^{SC} : Scooters capital recovery factor for N years at interest rate i
 A : Cost of the scooter management system in \$
 $\sum_{t=1}^{8760} P_L^{SC}(t)$: Scooter's annual discharged energy to supply load demand at time t
 $\sum_{t=1}^{8760} P_{trans}^{SC}(t)$: Scooter's annual discharged energy to supply transportation demand at time t
 E_{Grid} : Annual carbon emissions due to utility grid's purchased energy
 E_{Die} : Annual carbon emissions due to diesel generator energy in kg
 α : Tax on carbon emissions in \$/kg
 $P^{EDL}(t)$: Grid's purchased active power at time t
 $P^{Die}(t)$: Diesel's generator output power in Kw
 K_{CO_2-Grid} : Grid's carbon footprint in kg/kWh
 EFF : Emissions factor of fuel (diesel) in tons of CO₂-e/TJ
 L_{kwh} : Fuel consumption per kilo-watt hour of electricity in L/kWh
 NCV is the net calorific value of diesel in TJ/Gg
 D is the density of diesel in kg/L
 r : Scooter Service annual revenue in \$
 $CF_{charging}$: E-scooters and EVs annual charging cost in \$
 C is the charge rate of using an e-scooter in \$/km

$U(C)$: Cost-attractiveness function
 FT : Full transportation demand in km/hr
 $\lambda(t)$: Diesel Generator ON/OFF profile
 $x(t)$: BSS, EVs, and e-scooters charging profile
 $y(t)$: BSS and e-scooters discharging profile
 $y_{ev}(t)$: EVs discharging profile

CHAPTER 1

INTRODUCTION

The global increase in electric energy demand accompanied by the desire to boost green energy gave the world a wake-up call towards distributed generation (DG). DGs are small-scale generating or storage units connected to the utility grid at the distribution level posing by that a number of technical benefits to utilities, customers, and society [1]. DGs can be biomass-based generators, photovoltaic systems (PV), fuel cells, wind turbines, storage systems, etc. The ongoing evolution of renewable-based DGs, along with the emergence of the smart grid concept, coupled with the arising worries on energy security and fossil fuel energy reserves, have all contributed to paving the way toward microgrids (MGs).

MGs are a cluster of inter-connected loads and distributed energy resources (DERs) with well-defined electrical limits that operate as a single controllable entity with respect to the grid [2]. Hence, MGs generate, distribute, and regulate the flow of electricity to users similar to a standard grid, running in two basic operational modes: grid-connected or islanded mode [3]. Being characterized by uniqueness, diversity, controllability, interactivity, and independence, MG project implementations have significantly increased due to the MG ability in improving the network power quality, enhancing the reliability of the power supply, diminishing losses on transmission and distribution lines, and cutting the costs for extra power [4],[5]. Moreover, an indispensable contribution that a MG can provide as well, is its ability to deliver energy and guarantee continuous power supply to critical loads in case of large area blackouts

caused by either sudden accident, natural disasters, or previously planned blackouts [6], [7].

On the other hand, a new vital technology promoting sustainable development in climate change is the electrification of transportation. Electric Vehicle (EV) is a substitute transportation alternative that emits zero exhaust gases and produces minimal noise. Recently, the modernized power system governs three emerging concepts of grid-connected EV technologies which are the Vehicle to Microgrid (V2M), Vehicle to Vehicle (V2V), and Vehicle to home (V2H). Particularly, the Vehicle to Microgrid (V2M) concept permits the EV to improve the power system operation by allowing the energy exchange between the EV and the MG, thus providing numerous services to the MG. Consequently, this technology can be further classified into unidirectional and bidirectional. For unidirectional V2M, this approach exploits the communication between the MG operator and EV to control the charging of each EV in such a way the MG overloading, system instability, and voltage drop issues are avoided. Yet from the MG's perspective, the EV battery is considered not only an electric load but also an energy storage. Thus, the bidirectional V2M approach develops this concept to allow energy exchange between the EV battery and the MG for the aim of either charging the EV or supporting the MG's load. In this framework, integrating EVs with other energy systems presents a new opportunity to control power demand, reduce generation-load fluctuations, peak shave the consumption profile, and improve the reliability and sustainability of the power system [8]. EVs adoption has been supported mostly by governments and private sectors worldwide due to its ability to introduce significant enhancement of energy security by diversifying energy sources, encouraging economic growth by founding new

industries, and significantly reducing climate change crises by eliminating a considerable amount of green-house gases.

CHAPTER 2

LITERITURE REVIEW

To construct a low carbon economy and to create a sustainable power system, the integration of clean and renewable energy sources along with the adoption of EVs exhibits a crucial importance strategy. Consequently, a number of challenges will be posed in MGs in terms of managing DGs with the grid, controlling the charging of EVs, and exploiting the benefits of DGs in economy, energy, and environment. These main worries have drawn many scholars to target various aspects of these technologies.

2.1. Research Efforts on Determining the Optimal Configuration of a MG:

The MG concept is presented as a self-sustained network made up of DERs that can operate in an islanded mode during grid failures. However, solar and wind energy, in particular, are volatile and intermittent energy sources; therefore, energy storage systems are a must to overcome these uncertainties. In this context, the successful planning and deployment of MGs depend to a large extent on power sources selection and sizing [9]. Extensive research has been conducted to serve these problems. Wang et al. [10] aimed to find the optimal BSS size to smooth out the intermittent generation of the wind generator and achieve the highest economic benefit in terms of the power abstracted from the renewable source against the cost of the BSS installation. A similar problem was tackled by Kaldellis et al. [11] that considers the utilization of the maximum available solar energy together with an energy storage system in an autonomous small island. The obtained results clearly state that an optimum sizing combination of a PV generator along with an appropriate energy storage system can

considerably aid in minimizing the electricity generation cost in several island electrical systems, offering also abundant and high quality electricity without the environmental and macroeconomic impacts of the oil-based thermal power stations. Seddik et al. [12] proposed an iterative technique to find the optimal configuration of a grid-connected MG in terms of the number of PV panels and the capacity of BSS. The problem is formulated as a constrained optimization to reduce the annual cost of the system.

2.2. Research Efforts Related to EVs Adoption and Contribution in the Energy

Sector:

On the other hand, extensive research has been conducted to evaluate and foster the adoption of EVs in the energy sector and MGs particularly. In this sense, Karfopoulos et al. [13] outlined a hierarchical approach that allows efficient management of EV fleet load in such a way that the MG's technical constraints are not violated. This structure allows the participation of EVs in the electricity market. Thomas et al. [14] provided an energy management model for a university campus to assess the cooperation of several DG resources with the bidirectional energy exchange of EV fleet, which was used for work-related trips. Since the EV fleet consumes a high amount of energy, then it significantly modifies the load curve in a MG. Yoon and Kang [15] suggested an optimization algorithm intending to discover an optimal management scheme of a MG that maximally utilizes renewable energy resources while meeting EV charging demand (under controlled and un-controlled charging schemes). Case studies involving residential and campus MGs revealed an economic MG configuration with less CO₂ emissions.

On the contrary, the consideration of the EV fleet as a large storage capacity has also been addressed. Mortaz and Valenzuela [16] defined a mathematical energy management model in a grid-connected MG that aimed to minimize the operational costs by managing different sources of energy and efficiently exploiting EV in parking stations. Ioakmidis et. al [17] proposed a vehicle-to-building approach that peak-shave and valley-fill the power consumption of a building. The EMS developed aimed to optimally schedule the charging and discharging mechanisms of EVs, placed in large parking lots, such that the building power consumption profile was flattened to the greatest extent. In this fashion, Wang et al. in [18] had also shaped an EV control architecture for peak shaving and valley filling the consumption profile. By being implemented on real typical cities data, this approach had proven that as the number of EVs increases, the V2G expected load curve becomes closer to the target curve and hence the effectiveness of adopting the V2G system for this purpose is increased.

Research efforts to inspect cost interaction between EVs and renewable energy resources are brought in detail in the literature and can be figured out differently depending on various perceptions. Specifically, according to charging service providers, it aims to lessen operational costs and multiply revenues. Whereas for EV owners, it denotes the desire to drop the battery charging cost. As for the utility grid, it can involve electricity generation cost, system life span cost, and energy transmission costs. This has been validated in [19], [20] and [21].

2.3. Research Efforts Related to E-Scooters Service:

One of the most increasingly attractive segments in the EV market is light electric vehicles (LEVs) because they present a viable solution for short forms of

transport. LEVs which include e-scooters, e-bikes, e-rickshaws, e-forklifts, e-motorbikes, and low-speed EVs are easy to drive and handle [22]. With the introduction of LEVs, specifically e-scooters, coupled with the spread of smartphone-based services, the continuous increase in traffic congestion in cities, and the amount of private financing offered for green transportation services, shared micro-mobility gained much attention as they present an alternative for short trips, particularly to deliver first-mile-last-mile solutions for public transportation [23]. Numerous research studies showed the operations and use of these evolving shared micro-mobility systems that hold the promise for contributing to a more sustainable transportation system. Zuniga-garcia et al. [24] have analyzed e-scooters and transit trips in an urban area, and by using advanced spatial models they have investigated the factors affecting trip origins and destinations. This study was coupled with an evaluation of e-scooter usage in a university environment. Research efforts in [25], [26], and [27] have also analyzed competition between different shared micro-mobility modes of transport, by emphasizing on questions such as how and why specific services are used, in addition to their effect on urban mobility and its sustainability overall. As an instance, Reck et al. [28] estimated the first mode choice models between four different shared micro-mobility modes (dockless e-scooters, dockless e-bikes, docked e-bikes, and docked bikes) using vehicle location data. This methodology was applied to Zurich's largest and densest empirical shared micro-mobility dataset to date in Switzerland where results showed that the mode choice is nested and dominated by distance and time of day while docked modes are desired for commuting. Similarly, Campbell et al. [29] discussed factors that shape the choice of switching from a current transportation mode to bikeshare or e-bikeshare modes in Beijing by using a detailed preference survey.

Research on shared micro-mobility can be further classified into supply- and demand-side topics. These topics depend on features that influence demand which are internal features (i.e., user socio-demographics), external features (e.g., built environment, geography, weather), and trip-related features (destinations, distance, time of day). Munira et al. [30] showed that micro-mobility demand tends to be attributed to several demographic and socioeconomic factors. Buck et al. [31] explored a bikeshare system user travel behavior and formulated a profile of user demographics by comparing short-term (1 day) users and annual members of Capital Bikeshare (CaBi) in Washington, D.C. However, Degele et al. [32] make use of the large datasets on e-scooter customer's journey, scooter reservations, and the ride itself to understand customers' needs and goals. A customer clustering approach is then proposed that divides customers into four different categories defined by variable age, the time between rides, distance driven, and revenue per customer. This will allow several inferences to be drawn for business development and enhancing the problem-solution fit of the e-scooter sharing model. The need to forecast the demand for e-scooters trips has been addressed by Lee et al. [33]. The log-log regression demand model was formulated based on user age, income, labor force participation, and health insurance coverage. Moreover, Habib et al. [34] studied the effects of seasonal variations in terms of weather, land use, sociodemographic variables, and built environment attributes on Bike share in Toronto using a regression analysis that relied on three different levels: trip generation, trip attraction, and station-to-station trips. In this context, Bachand-Marleau et al. [35] surveyed Montreal to define the factors that fostered individuals to use the bike share system and the elements that influenced the frequency of use. Results

showed that the location of docking stations was an important aspect for encouraging users to utilize shared bicycles.

Provided that the travel behavior does not always mirror experiences and satisfaction, several research efforts aim to analyze the user's satisfaction level through different methods. One of the most important approaches adopted in literature was conducting user surveys by collecting ratings given by users to certain aspects of the system like convenience, safety, accessibility, affordability, etc. [36]. Knowing user's needs and preferences together with the potential dimensions of a particular service will facilitate planning, operation and help investors focus on attributes that travelers need. For instance, Del Castillo et al. [37] proposed three models to present users' preferences: a model based on means, a model based on a multivariate discrete distribution, and a generalized linear model that tied the relation between global satisfaction rating and the specific satisfaction ratings. Those were based on questions asked to users on different features of the transportation system. On the other hand, Imam [38] conducted a user survey to discover the satisfaction of bus users, minibus users, and jitney users for the aim of reducing private car use in the future. Abenoza et al. [39] recognize and characterizes current and potential users of public transport in Sweden as well as explored the most crucial factors of travel satisfaction with Public Transport services for different segments of travelers. Almannaa et al. [40] studied the feasibility of launching an e-scooter sharing system in Riyadh, Saudi Arabia by conducting a survey that aims to shed the light on the insights of the integration of such a system in the city and the willingness of users to use such a service.

2.4. Research Efforts on MGs EMS and Its Associated Optimization Techniques:

As a matter of fact, a MG requires an EMS for optimal use of all distributed energy resources in an intelligent, secure, reliable, and coordinated way. An EMS includes both supply and demand-side management [41]. However, with the different combinations of renewable energy resources, energy storage systems, EVs, and demand response, the MG's EMS strategies have been diversified from economic dispatch to unit commitment. The other strategies are scheduling of DERs and loads, minimization of system losses and outages, control of intermittency and volatility of renewable energy resources, and realization of economical, sustainable, and reliable operation of MG [42]. However, some of these problems involve large numbers of nonlinear variables. Numerous review papers solved such EMS problems by utilizing different optimization techniques. Some authors used EMS based on linear and non-linear programming methods as in [43],[44]. Others used EMS based on dynamic programming and rule-based methods as in [45],[46]. Yet, different heuristic approaches emphasizing mostly on particle swarm optimization (PSO) and genetic algorithm have been applied [47],[48]. On the other hand, many authors utilized different convex optimization approaches and relaxations in this field like semi-definite programming, geometric programming, duality, quadratic programming, etc. [49]–[53].

CHAPTER 3

PROBLEM FORMULATION

The energy sector in Lebanon is run by the Electricité du Liban (EDL), an independent power utility, whose mission is to generate, transmit, and distribute electricity to all Lebanese territories. However, the Lebanese electric power sector has been dealing with several challenges throughout the years. Starting with the outbreak of the civil war (1975 until 1990) which has ruined the electricity sector and dropped it behind the global and regional energy trends, results in massive destructions in the electricity infrastructure. This is followed by a set of problems on the country level involving political instabilities, corruptions, weak and inefficient electricity production, aging of power plants, technical losses in the transmission and distribution networks, and main reliance on fuel-based electricity. The problem is set to worsen with the increase in population that took into account the Syrian refugees who surge the electricity demand, as the country welcomed over 1.5 million immigrants in the last few years. As a result, the gap between the demand and the supply enlarges to leave the Lebanese people with a nearly 1300-1600 MW power shortage. The effects of this problem are obvious in the daily blackouts that are scheduled sometimes and differ from one region to another. Yet challenges expanded further to reach the economic and financial collapse that Lebanon is encountering these days [54], [55].

The complete reliance on fuel for electricity production presents the fundamental problem for this crisis because of the vast increase in oil prices over the years coupled with the lack of tariff adjustment (since 1996). Imported fuels account for nearly a quarter of the national budget deficit. The latter results in production costs

being uncovered thus setting Lebanon's power supply in some major power shortages the can reach 20hrs/day in some regions. This intermittent power supply has driven private electricity providers to play a crucial role in supplying demand during grid outages by using diesel generators as a main alternative energy resource. Unfortunately, the use of these standby diesel generators comes with a health and environmental cost since they can cause local air quality degradation especially when it emits excessive greenhouse gas emissions in absence of proper and periodic maintenance [56].

Moreover, as Lebanon continues to cope with the currency crisis that presents a serious threat to drive the country, which is already on shaky economic ground, into complete bankruptcy, it is hard to develop a solution in these difficult circumstances. Thus, the purpose of this research is to reshape the power supply system of the American University of Beirut (AUB) campus, currently characterized by consistent daily grid blackout hours, by shifting the electricity deficit to clean DERs, rather than the heavy reliance on on-site diesel generators. This desire arose as an attempt to build up a reliable source of energy given that diesel is one of the imported fuels and thus not being always available as well as being subjected to volatile prices and international public regulations and sanctions. So to seek a solution beyond diesel generators with the aim to convert AUB campus to a green sustainable one, the goal is to enhance campus energy security, reduce site emissions and diminish power purchased at peak tariff hours by combining several clean energy resources. These sources include a PV system and BSS. In addition, we proposed the usage of EVs as a substitute to conventional fuel-based vehicles used for work-related trips on one hand, and its use as a battery storage system after fulfilling their transportation demand on the other hand. Moreover, this work aims to optimize the operation of the integrated DERs and efficiently manage

the EV fleet by connecting the campus to the utility grid under normal regular operation and having the DERs responsible for supplying load demand during scheduled blackouts. Besides, this study will also examine the feasibility of integrating an e-scooter sharing system to aid AUB community to commute easily on campus that exhibits an area of 250,000 square meters. Despite its preliminary function, this sharing system could play a significant role in supplying load demand by acting as a virtual battery storage system in the absence or lack of a large commuting demand as in vacations, holidays, weekends, etc.

Therefore, to achieve the mentioned targets, two main optimization stages are implemented. The first is a multi-objective optimization problem formulated to converge to an optimal PV/BSS configuration and to an optimal charge rate to be imposed on using e-scooters service. This goal is attained by optimizing a rule-based EMS using two distinct optimization methods: particle swarm optimization (PSO) and FMINCON via YALMIP parser. This level will converge to the optimal decision variables while ensuring an efficient reliable secured source of energy, diminishing carbon footprint through reducing diesel dependency, and reducing the total cost of the MG in terms of operation and investment. The second optimization stage takes the optimally configured MG and optimizes its operation via an optimal EMS. In this case, the convex optimization method has been utilized to find the MG's optimal performance.

CHAPTER 4

SYSTEM MODELLING

To achieve fruitful results, the design of a MG should exploit greatly DGs benefits that cannot be achieved without proper modeling for each source. Thus, the modeling of the energy sources and demand in the MG under consideration consists of solar PV array, BSS, diesel generators, grid, in addition to EVs, e-scooters, and their associated transportation demand.

4.1. Photovoltaic Modelling:

Being abundant and free, sunlight is considered an efficient source of energy that can be directly converted into electric energy by the use of PV panels. The output power generation from this renewable source of energy fluctuates as it is highly affected by varying meteorological conditions that include mainly solar irradiance and operating temperature. A standard PV module converts 6-20% of the incident solar irradiance into electricity. The remaining incident solar irradiance is converted into heat that causes a rise in the temperature of the PV module cells and consequently a significant reduction in the PV module output power [57]. An accurate assessment of the PV system performance considers these ecological parameters. Thus, the AC PV instantaneous output power is expressed by the following equations [58]:

$$P^{PV}(t) = FF(t) \times I_{sc}(t) \times V_{oc}(t) \times \eta^{PV} \quad (1)$$

$$\text{where, } I_{sc}(t) = \frac{S}{S_{STC}} [I_{sc,STC} + K_i(T_c(t) - 25)]$$

$$V_{oc}(t) = V_{oc,STC} - K_v \times (T_c(t) - 25)$$

$$FF(t) = FF_0(t) \times [1 - r_s(t)]$$

$$\begin{aligned}
FF_0(t) &= \frac{V_{oc,0}(t) - \ln[V_{oc,0}(t) + 0.72]}{V_{oc,0}(t) + 1} \\
V_{oc,0}(t) &= V_{oc}(t) \times \frac{q}{nk[T_c(t) + 273.15]} \\
r_s(t) &= R_s \frac{I_{sc}(t)}{V_{oc}(t)} \\
T_c(t) &= T_a(t) + s \frac{NOCT - 20}{0.8} \\
R_s &= R_{s,STC} = r_{s,STC} \frac{V_{oc,STC}}{I_{sc,STC}} \\
r_{s,STC} &= 1 - \frac{FF_{STC}}{FF_{O,STC}} \\
FF_{STC} &= \frac{V_{mppt,STC} \times I_{mppt,STC}}{V_{oc,0,STC} + 1} \\
FF_{O,STC} &= \frac{V_{oc,0,STC} - \ln[V_{oc,0,STC} + 0.72]}{V_{oc,0,STC} + 1} \\
V_{oc,0,STC} &= V_{oc,STC} \times \frac{q}{nk[T_{c,STC} + 273.15]}
\end{aligned}$$

where, $I_{sc}(t)$ and $V_{oc}(t)$ are the short circuit current and open-circuit voltage under operating conditions, s is the solar irradiance in kW/m^2 at any time t , $FF(t)$ and $FF_0(t)$ are the actual and ideal fill factor of the module. $V_{oc,0}(t)$ is the normalized open-circuit voltage at any time t , q is the charge of an electron, n is the ideality factor assumed equal to 1, k is Boltzmann's constant, $T_c(t)$ is the module's temperature at any time t in $^\circ\text{C}$, R_s is the module series resistance, $r_s(t)$ is the normalized module series resistance at any time t , $T_a(t)$ is the module ambient temperature and NOCT is the nominal operating cell temperature provided by the manufacturer. η^{PV} is the efficiency of the PV inverter. $r_{s,STC}$ is the normalized series resistance under standard test conditions (STC), FF_{STC} and $FF_{O,STC}$ are the actual and ideal fill factor under STC, respectively. $V_{oc,0,STC}$ is the normalized open circuit voltage under STC.

The hourly annual ambient temperature and solar irradiance data profiles collected at AUB university campus during the year 2017 are illustrated in Figures 1

and 2, respectively. The accurate measurements of the ambient temperature for the selected site show that the highest temperature was recorded during the summer season at 38°C in July. Additionally, the maximum and minimum values of solar irradiance are 966.54 w/m^2 and 1.78 w/m^2 recorded on the 27th of July and the 9th of January, respectively. The amount of solar irradiance received by the campus area is relatively good, which denotes that the PV system is an attractive power source of energy.

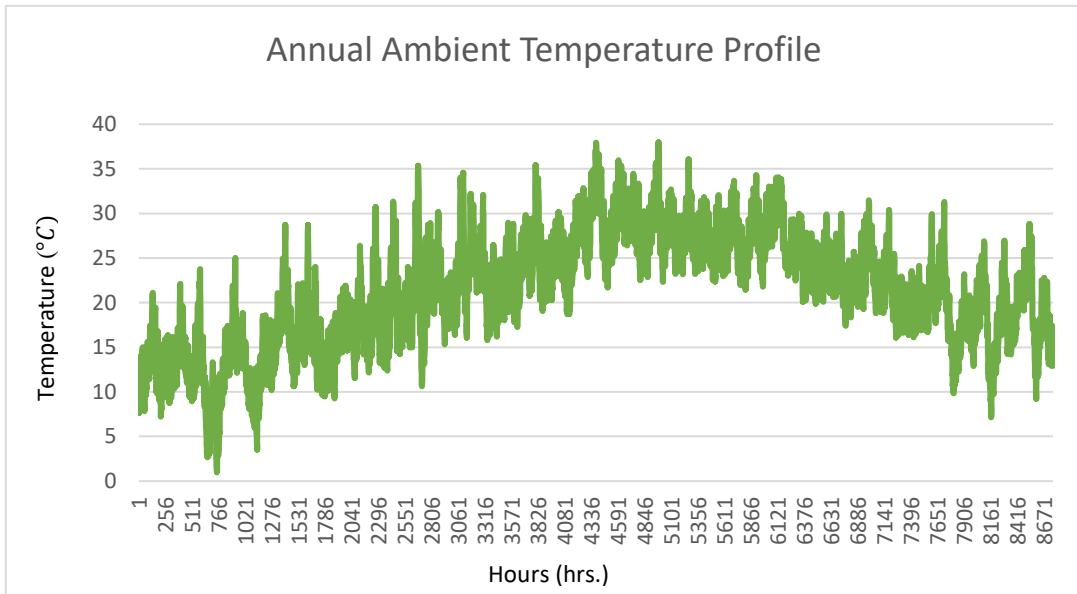


Figure 1: Annual ambient temperature profile of AUB campus during the year of 2017.

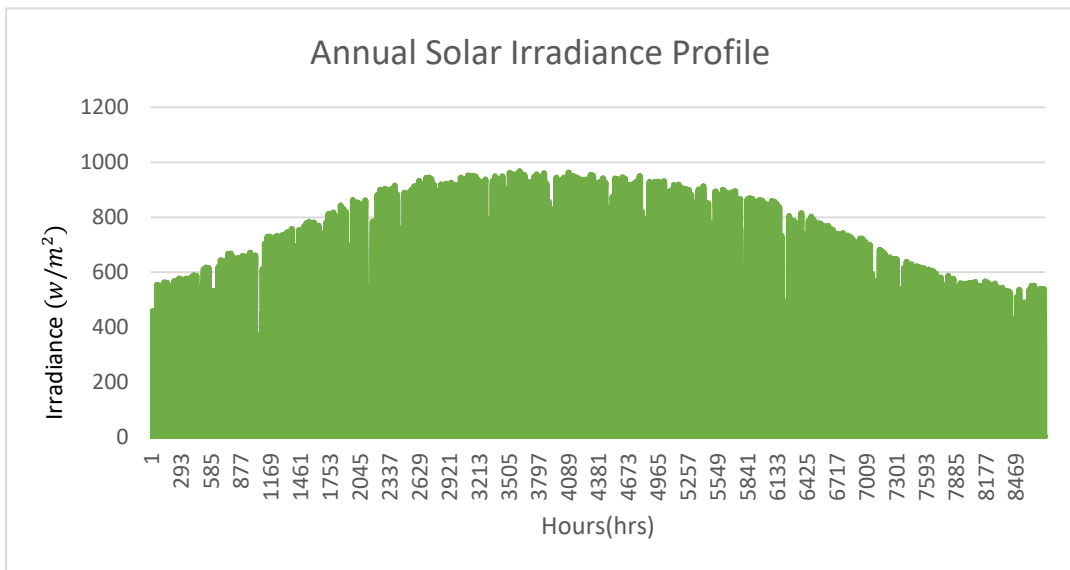


Figure 2: Annual solar irradiance profile of AUB campus during the year of 2017

The chosen PV module to be installed at AUB campus site is LC365Q1C-A5 [59]. This module has an efficiency value of 21.1 % which is considered to be high in comparison to the efficiencies of the most PV modules available today in the market (15-18%) [60]. Efficiency matters since it is a significant sign of the overall module quality. The full specifications of this module are depicted in Table 1.

Table 1:PV module characteristics	
LG365Q1C-A5	
Rated Power (w)	365
$V_{OC,STC}$ (v)	42.8
$I_{SC,STC}$ (A)	10.8
$V_{mppt,STC}$ (v)	36.7
$I_{mppt,STC}$ (A)	9.95
NOCT(°C)	44
K_v (v/°C)	-0.10272
K_i (A/°C)	4.00E-03
Dimensions (mm3)	1700 x 1016 x 40
Module Efficiency (%)	21.1
Inverter Efficiency (%)	95

Taking into account the solar irradiance and ambient temperature data profiles along with the characteristics of the selected PV module, the annual PV output power calculated using equation (1) is illustrated in Figure 3.

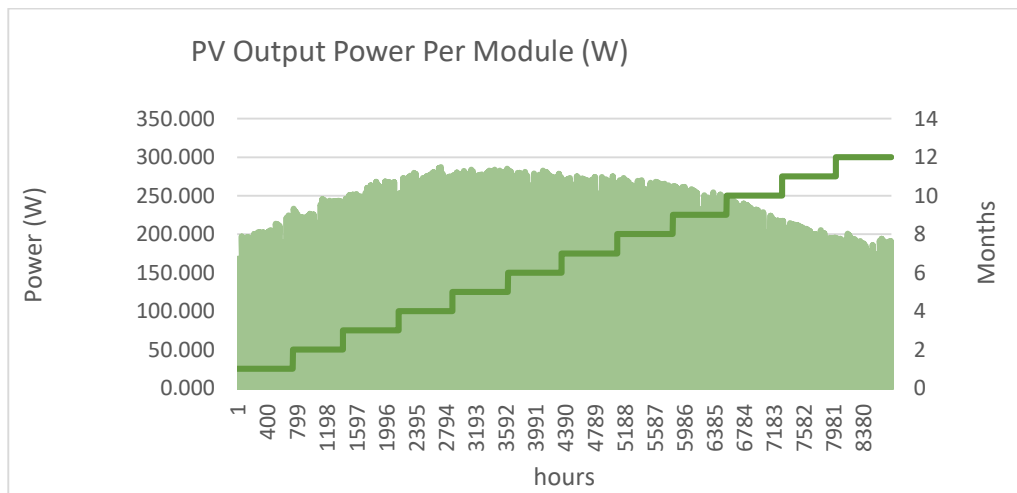


Figure 3: Annual PV output power per module.

Considering the goal of decreasing the costs of operation and investment of the PV system, the PV economic model has the same importance as that of the electrical one. The principal economic element is the PV system cost of energy which is the annual average cost per kWh of producing electricity. This total annualized cost is a function of the capital cost and its operation and maintenance (OM) cost. These are described by the following set of equations [61]:

$$CC^{PV} = f(P^{PV,r}) \quad (2)$$

$$OM^{PV} = f(P^{PV,r}) \quad (2)$$

$$AP^{PV} = CC^{PV} \times CRF^{PV}(i, N) + OM^{PV} \quad (3)$$

$$\text{where } CRF(i, N) = \frac{i(1+i)^N}{(1+i)^N - 1}$$

$$COE^{PV} = \frac{AP^{PV}}{\sum_{t=1}^{8760} P^{PV}(t)} \quad (4)$$

where, $P^{PV,r}$, CC^{PV} , OM^{PV} , AP^{PV} , $CRF^{PV}(i, N)$ and COE^{PV} are PV system's rated capacity in kW, capital cost in \$, operation and maintenance cost in \$/year, annual loan payment in \$, capital recovery factor and cost of energy in \$/kWh, respectively.

4.2. EDL (Grid) Modelling:

Traditionally, the utility grid is considered to be the major power supply available to communities and so is the case for the MG under study. However, AUB campus operates in an unreliable grid set-up as it is characterized by daily scheduled blackouts. Such blackouts are illustrated in Table 2, where 69% of the daily blackout durations are planned for 3 hours, 14% for 4,5,6, and 7 hours' outage durations, and 17% for no outage at all.

Table 2: Scheduled daily grid's outage	
Blackout Timing #1	07:00 am to 10:00 am
Blackout Timing #2	10:00 am to 13:00 pm
Blackout Timing #3	13:00 pm to 04:00 pm
Blackout Timing #4	04:00 pm to 07:00 pm

The loads connected to this grid are subjected to a grid's triple tariff rate scheme: night tariff, mid-day tariff, and peak tariff (Table 3). The latter possesses the highest price of electricity usage 0.213\$/kWh corresponding to the evening time.

Table 3: Grid's triple tariff rate scheme	
Night Tariff	0.053 \$/kWh
Mid-day Tariff	0.073 \$/kWh
Peak Tariff	0.213 \$/kWh

Grid's purchased power is formulated as shown by the following equation:

$$P^{EDL}(t) = EDL_{profile}(t) * P^{edl}(t) = \begin{cases} P^{EDL}(t) & \text{for } \Phi = 1 \\ 0 & \text{for } \Phi = 0 \end{cases} \quad (6)$$

where, $P^{EDL}(t)$ is the power supplied in kW by the grid at time slot t , and

$EDL_{profile}(t)$ is a binary decision variable that represents the grid state (ON/OFF) at time t .

4.3. Battery Storage System (BSS) Modelling:

The BSS is used either to store the excess energy production from the PV system or to store energy purchased from the utility grid at its lowest tariff rate (night tariff rate). BSS will deliver this stored energy during the grid's outage or peak tariff rate hours. The modeling of the BSS output power is expressed by the following set of equations [62]:

$$P_{ch}^{BSS}(t) = \frac{P_{DC}^{BSS}(t)}{\eta^{BSS}} \quad (7)$$

$$P_{dch}^{BSS}(t) = P_{DC}^{BSS}(t) * \eta^{BSS} \quad (8)$$

$$P_{DC}^{BSS}(t) = \frac{E^{BSS}(t) - E^{BSS}(t - \Delta t)}{\Delta t} \quad (9)$$

$$SOC(t) = \begin{cases} SOC(t - \Delta t) \times (1 - a) + \eta^{BSS} \frac{P_{ch}^{BSS}(t)}{C^{BSS} \times V \times SOH(t)} \Delta t \\ SOC(t - \Delta t) \times (1 - a) + \frac{P_{dch}^{BSS}(t)}{\eta^{BSS} \times C^{BSS} \times V \times SOH(t)} \Delta t \end{cases} \quad (10)$$

where, $P_{DC}^{BSS}(t)$ is the DC charging/discharging rate of the battery in kW. $P_{dch}^{BSS}(t)$ is the AC discharging power of the battery in kW, $P_{ch}^{BSS}(t)$ is the AC charging power of the battery in kW and η^{BSS} is the BSS inverters efficiency. $E^{BSS}(t)$ is the battery energy in kWh. $SOC(t)$ is the state of charge of the battery at each time t , C^{BSS} is the nominal capacity in Ah, V is the battery nominal voltage, a is the self-discharging factor, SOH is the battery's state of health. SOH is an important factor to consider in modeling the BSS because it provides critical information about BSS performance and lifetime. The BSS SOH is computed by taking into account the impact of the energy discharged on batteries' capacities. Table 4 provides SOH relation as a function of the BSS discharged energy. A polynomial function representing SOH in terms of the discharged energy is used to describe the batteries' energy retention during the first 10 years.

Year	Aggregated Discharge (kWh/year/kWh)	Minimum Retention	Yearly Energy Output
1	348	95%	348
2	679	91%	331
3	996	88%	317
4	1302	83%	306
5	1599	79%	297
6	1889	77%	290

7	2173	75%	284
8	2451	73%	278
9	2725	71%	274
10	2994	70%	269

To minimize the BSS cost of operation and investment, the equations underlying the dynamics of the BSS economic model in terms of capital cost, operation and maintenance costs, and charging cost are presented below:

$$CC^{BSS} = f(P^{BSS}, r) \quad (11)$$

$$OM^{BSS} = f(P^{BSS}, r) \quad (12)$$

$$AP^{BSS} = CC^{BSS} \times CRF^{BSS}(i, N) + OM^{BSS} \quad (13)$$

$$COE^{BSS} = \frac{AP^{BSS} + \sum_{t=1}^{8760} P_{ch}^{BSS}(t) \times EDL_{Tariff}(t) + \sum_{t=1}^{8760} P_{ch}^{BSS}(t) \times \eta^{BSS} \times COE^{PV}}{\sum_{t=1}^{8760} P_{dch}^{BSS}(t)} \quad (14)$$

where AP^{BSS} , CC^{BSS} , and OM^{BSS} are the BSS annual loan payment in \$, BSS capital cost in \$ and operation and maintenance cost in \$/year, respectively. Whereas, COE^{BSS} is the BSS cost of energy in \$/kWh and $EDL_{Tariff}(t)$ is the grid electricity tariff at time t in \$/kWh.

4.4. Electric Demand Modelling:

Figure 4 shows the power consumption profile (in MW) of AUB's campus as in 2017. Note that the power demand is subjected to variations on a seasonal, weekly, and daily basis. Summer days exhibit the highest electricity demand reaching a peak value of 12.08 MW in August.

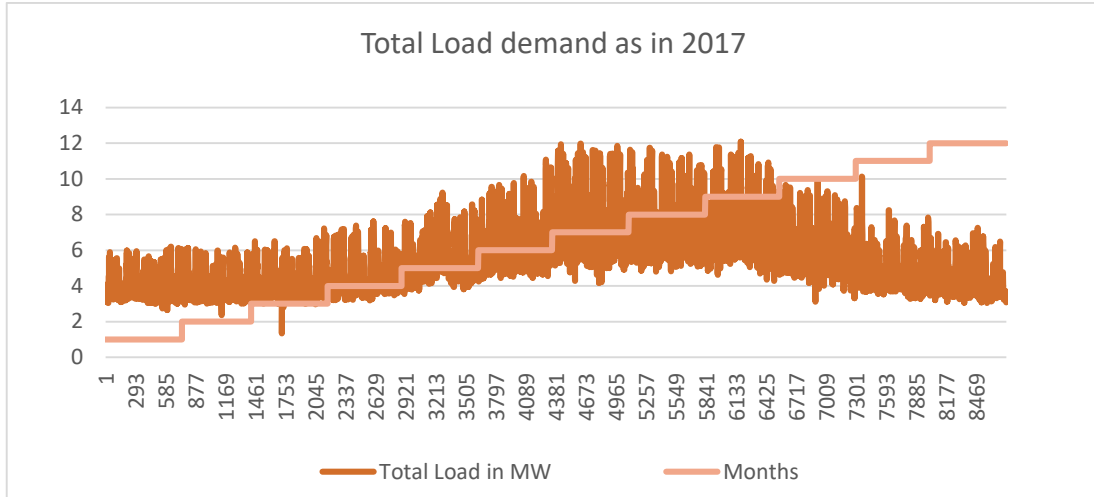


Figure 4: AUB annual load demand profile as in 2017

The annual electricity demand of AUB is usually covered by the diesel generators during blackouts and the utility grid under regular operation. This is illustrated in the following table:

	Grid	Diesel Generator	Total
Annual Energy Demand (MWh)	30,208	16,335	46,544

4.5. Diesel Generator Modelling:

The nature of electric energy generation from renewable energy resources deployed in the proposed design depends highly on resource availability (solar irradiance). So, the AUB campus will remain relying to a great extent on diesel generators to supply load during grid outages. Thus, diesel generators will still act as the primary backup source of energy to supply and meet the load demand.

Diesel generators are modeled by the following set of equations [63]:

$$FC(t) = \gamma P^{Die}(t) + \beta P^{Die,r} \quad (15)$$

$$CF(t) = FC(t) * \psi(t) \quad (16)$$

where, $FC(t)$ is the fuel consumption in L at time t , $P^{Die}(t)$ and $P^{Die,r}$ are the actual output power and rated power of the diesel generator in Kw, respectively. γ and β are fuel consumption coefficients, $CF(t)$ is the diesel fuel cost of the diesel generator in \$ at time t and ψ is the diesel cost in \$/L at time t .

The diesel generator plant installed at AUB consists of 5 different types of generators mounting to a total of 13 and forming a total capacity of 15,300 kW. These five different types along with their associated capacities are described in Table 6.

	Capacity (kVA)	Capacity (kW)	No. of Sets
Caterpillar 3608	2000	1600	3
MTU	2500	2000	1
Ruston 12CVA	750	600	4
Caterpillar C32	875	700	3
Caterpillar C175	2500	2000	2

The cost of energy from diesel generators describes their economic model. This cost is expressed as the ratio of the operation and maintenance costs to the annual generated energy. This is illustrated by the below equations:

$$OM^{Die} = f(P^{Die,r}) \quad (17)$$

$$AP^{Die} = OM^{Die} \quad (18)$$

$$COE^{Die} = \frac{AP^{Die}}{\sum_{t=1}^{8760} P^{Die}(t)} \quad (19)$$

4.6. Electric vehicle (EV) Modelling:

The MG understudy owns 59 work-related trip vehicles and are divided into several classes: busses, cars, vans, and passenger EVs which are used by employees for

transportation. Whereas, pick-ups and trucks are used for general work-related trips. The different types and quantities are described in Table 7.

Table 7: AUB service vehicles data		
Types	Quantities	Department
Vans	13	Biology- IT- Physical Plant- Dietary services-AREC, etc.
Busses	3	Physical Plant, Chief Financial Officer
Pick-ups	11	Laundry- AREC- Physical Plant,etc.
Cars	26	President's Office, Housing, Protection Office, Admission Office, Chief financial Officer, etc.
Truck	2	Environmental Health Safety and Risk Management (EHSRM) , Physical Plant.
Passenger EVs	4	EHSRM, Physical Plant
Ambulance	1	Protection Office

Conventional vehicles which create a major source of CO₂ emissions are replaced by electrical ones. These EVs are chosen in such a way that their batteries can accomplish their associated work targets on one hand, and can supply partial load demand during peak tariff hours on the other hand. The batteries forming the EV fleet have a total capacity of 2.83 MW. This is depicted in Table 8.

As a result, the EV parking lot is assumed to be a single virtual battery storage with a capacity that depends on the number of different battery capacities of the available EVs in it. This lot is provided with a bidirectional flow capability so that EVs can function in both directions as either vehicle to microgrid (V2M) or microgrid to vehicle (M2V).

Table 8: Proposed AUB electric service vehicles		
Types	Quantities	Battery Storage (kWh)
BMW I4 [64]	1	80
Chevrolet Bolt EV 2020 [65]	3	66
Ford Transit 350HD Cargo Van [66]	1	43
FUSO eCanter [67]	1	82.8

Jeep Renegade TRAILHAWK 4xe	3	11.4
KIA e-Niro [68]	5	64
Mercedes e-Sprinter [69]	2	55.2
Nissan Dongfeng Rich 6 EV [70]	4	68
PEUGEOT e-208 50 kWh Active 136 Auto [71]	8	50
Peugeot Partner Electric van [72]	5	22.5
R1T TRUCK [73]	1	105
Renault Kangoo Maxi ZE 33 [74]	3	33
Tesla Model S [75]	1	70
YTEV Bus [76]	1	258
YTEV Mini Bus [77]	3	66
Total Capacity	42	2,383

Since EVs are considered to be dynamic energy storage, so they are also governed by the set of equations provided in the BSS modeling section. However, its economic model is a function of the EVs capital costs and cost of charging, this is described by the following set of equations:

$$CC^{EV} = \sum_{i=1}^{42} EV(i) \times CC(i) \quad (21)$$

$$AP^{EV} = CC^{EV} \times CRF^{EV}(i, N) \quad (22)$$

$$COE^{EV} = \frac{AP^{EV} + \sum_{t=1}^{8760} P_{ch}^{EV}(t) \times EDL_{Tariff}(t)}{\sum_{t=1}^{8760} P_L^{EV}(t) + \sum_{t=1}^{8760} P_{trans}^{EV}(t) * \eta^{EV}} \quad (23)$$

where, CC^{EV} is the total capital cost of the EV fleet in \$, $CC(i)$ is the capital cost of $EV(i)$ in \$, CRF^{EV} is the EVs capital recovery factor for N years at interest rate i , $\sum_{t=1}^{8760} P_L^{EV}(t)$ is the annual discharged energy to supply load demand in kW, and $\sum_{t=1}^{8760} P_{trans}^{EV}(t)$ is the annual discharged energy to supply transportation demand.

As a matter of fact, AUB already owns a few EVs used by the physical plant, EHSRM, and PCA. Thus, the charging techniques already adopted will be used to charge the new fleet without introducing new charging stations.

4.7. E-Scooters Modelling:

Micro mobility services revealed an exponential growth in recent years due to the introduction of shared electric scooter (e-scooter) services that have emerged as a primary alternative for short trips. Since AUB campus size is about 250,000 square meters, bringing such a service can effectively aid AUB community to commute easily. However, this service will be integrated in parallel to the campus rules and guidelines to ensure proper scooter operation and user safety. This requires e-scooter riders to use them only in the allowed lanes. Scooters can be parked only at e-scooters stations. Also, the maximum e-scooter speed will be limited to 16 km/h. Failure to follow the university regulations will result in extra costs assigned to the corresponding user. Table 9 illustrates the electrical and safety characteristics of the e-scooter chosen. This scooter has been selected based on its large battery capacity so that it can supply its daily forecasted transportation demand primarily and supply partial load demand when EDL is OFF or/and during peak tariff hours secondly.

Table 9: E-scooter safety and electrical characteristics		
Hangzhou Fitcoo: FITRIDER T2S [78]		
Battery	Type	Swappable LG 16Ah – 576 Wh
	Lock	Available
	Nominal Voltage	36 v
	Max. charging Voltage	42 v
	Fuse	Available
	Battery Management System	Over-discharge protection....
	Typical Range	60-65 km
	Shock Absorption	Front fork Shock-absorption
	Brake	Front and rear drum brake
	Charging Time	3-5 hrs.
	Light	Built-in LED light, Tail Light
	Ring Bell	Available
	Dimensions (cm)	117x18.5x120

Since the sustainability of this micro-mobility service system depends highly on the scooter network connectivity and accessibility, the e-scooter charging/docking stations are thus spread across AUB campus according to Figure 5. In this fashion, users entering any of the AUB gates can directly use a scooter to reach his/her destination. As for the remaining stations, they were chosen according to the space availability in such a way each point can connect several user destinations. The electrical and security specifications of the chosen charging/docking station are illustrated in Table 10.

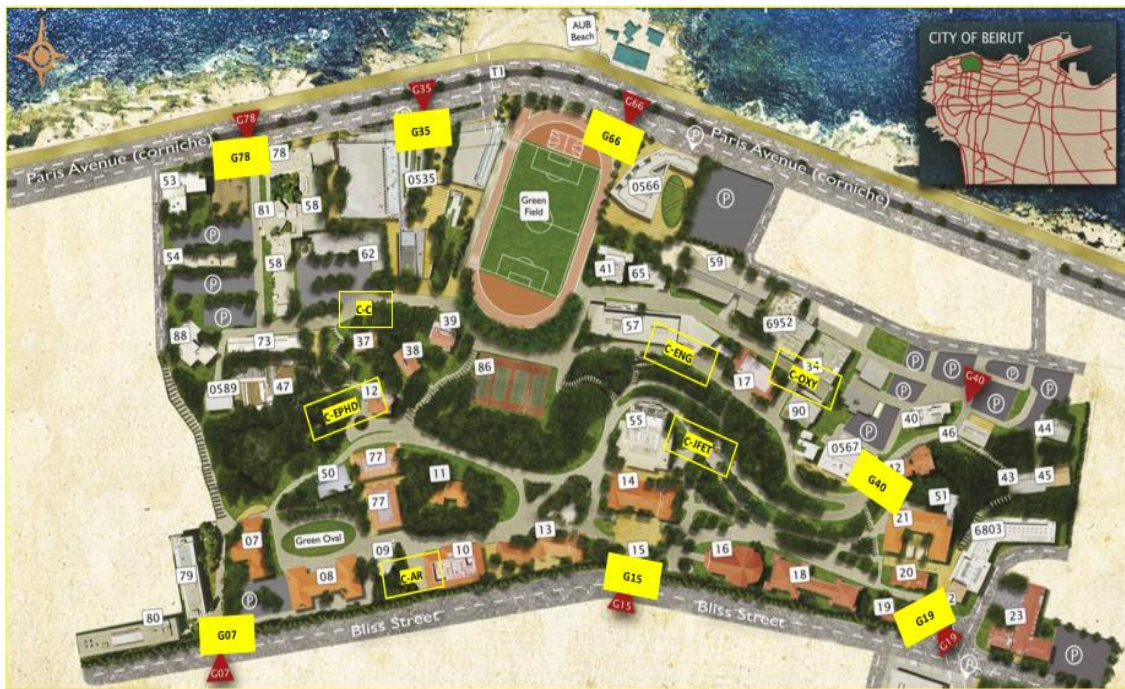


Figure 5: Location of the e-scooters charging/docking stations

Table 10: E-Scooters charging/docking stations specifications	
Hangzhou Fitcoo Station [79]	
Input Voltage	AC 100-240v/50-60Hz
Output Voltage	42 v DC
Length	3 m
Unlocking Time	1-2 sec
Unlocking Method	Scan QR Code, License Number, APP...
Safety Protection	Earth leakage protection, Anti-moist,....
Charging Indicator	
Error Alarm	
Buzzer	

Smart Lock
Over-Charging protection

Additionally, the e-scooters will be unlocked electronically (using IDs, membership cards, etc.). Charging dollars for e-scooters usages will stop after they are locked in any of the nearest e-scooter stations. Each trip will be charged in proportion to the distance covered by the user to reach his/her destination (dollars/kilometer). Payment methods include: subscription (pay a weekly or monthly subscription based on "x" amount of kilometers) or pay per use (pay first and then consume them per single ride). To efficiently manage this shared public service at AUB, a scooter management system is integrated that will provide information regarding scooters' locked/unlocked statuses, batteries charge level, and scooter location. In addition to that, this system can also provide ride details in terms of ride date and duration, user ride information, ride trajectory (speed, GPS, distance, charge rate \$/km), as well as geofencing properties like parking zones availability, speed limit zones and scooter position per second, this can help users change their origin or destination in advance if they knew *a priori* that the station would be full [80],[81].

Being considered as dynamic energy storages, e-scooters are governed by the set of equations provided in the BSS modeling section (section 4.3). However, its economic modeling is described by the following set of equations:

$$OM^{SC} = f(N^{SC}) \quad (25)$$

$$CC^{SC} = f(N^{SC}) + f(N^{Station}) + A \quad (26)$$

$$AP^{SC} = CC^{SC} \times CRF^{SC} + OM^{SC} \quad (27)$$

$$CRF^{SC} = \frac{i(1+i)^N}{(1+i)^N - 1} \quad (28)$$

$$COE^{SC} = \frac{AP^{SC} + \sum_{t=1}^{8760} P_{ch}^{SC}(t) \times EDL_{Tariff}(t)}{\sum_{t=1}^{8760} P_L^{SC}(t) + \sum_{t=1}^{8760} P_{trans}^{SC}(t) \times \eta^{SC}} \quad (29)$$

where, N^{sc} and $N^{Station}$ are the number of e-scooters and charging/docking stations to be integrated, CRF^{SC} is scooters capital recovery factor for N years at interest rate i , A is the cost of the scooter management system in \$, $\sum_{t=1}^{8760} P_L^{SC}(t)$ is the annual discharged energy to supply load demand, and $\sum_{t=1}^{8760} P_{trans}^{SC}(t)$ is the annual discharged energy to supply transportation demand.

4.8. Electric Vehicle Transportation Demand Modelling

Based on AUB databases, the fuel consumption of each conventional vehicle is estimated on yearly basis. Thus, the daily transportation trip distance (in km/day) that each vehicle usually covers is calculated based on the fuel consumption rate per kilometer associated with each type of vehicle. Afterward, this obtained value (km/day/conventional vehicle) is converted to transportation energy demand given the range and battery capacity of each EV.

However, it was recognized that not all vehicles are supposed to work on a daily basis. This is depicted in Figure 6, where 35% of the vehicles works on a daily basis, 28% works for 6 days/week, 21% works for 2 days/week, 7% works for 5 and 4 days/week, and 2% corresponding to 3 working days/ week.

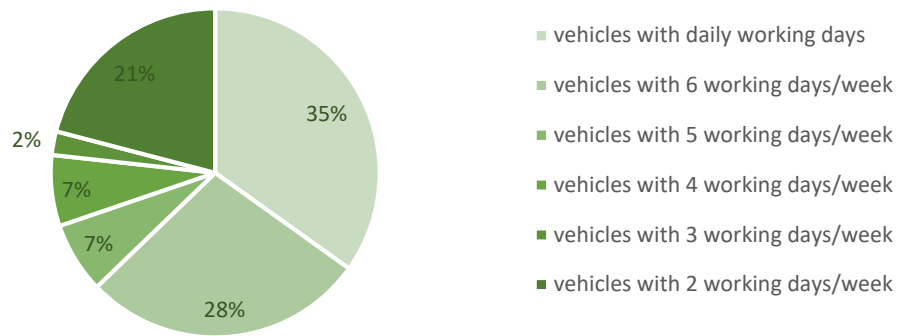


Figure 6: Frequency of the work-related trips covered by the service vehicles expressed in days per week.

The daily EVs transportation demand is formulated based on the fuel consumption of the conventional vehicles per day and their working days per week. Thus, the total weekly energy demand for transportation is depicted in Table 11 such that a 25 % excess energy of this demand is being reserved for urgent trips or unexpected trip delays.

Monday	Tuesday	Wednesday	Thursday	Friday	Saturday	Sunday
474	298	474	265	237	209	77

Besides the fact that the EV batteries are modelled to fulfill the daily work-related trips, they are also used to discharge their daily excess energy to supply load at the end of their duty hours.

4.9. E-Scooter Transportation Demand Modelling:

Shared e-scooters are a relatively recent addition to the shared micro-mobility mix. The need to forecast and analyze a micro-mobility sharing service demand is an essential primary step before making any investment decision. However, there is a direct link between the actual service and the customer's opinion of it. Therefore, for

the aim of attracting a large number of users, the service should be customer-oriented and consequently be designed and performed in a way that meets the levels of satisfaction required by users. In fact, the user satisfaction level in a public transport system is considered to be an aggregate measure of the satisfaction perceived by the user for various features of the sharing system. In what follows, the overall satisfaction will be called ‘global satisfaction’. Particularly, the most crucial aspects that influence this level are trip duration, service accessibility, fare, network connectivity, comfort and safety measures.

The e-scooter transportation demand and the total quality of the e-scooter project which to be integrated at AUB have been directly determined through a user survey. This survey targets AUB campus community which encompasses 11,924 personnel, including faculty members, employees, and students as described in Table 12. The conducted survey sample accounted for approximately 1.5% of the population and is completely random in such a way the rate of response was not controlled. Survey detailed findings and their associated statistical analysis are explained in appendix.

Table 12: AUB population data	
Total Number of Students	9408
Total Number of Faculty Members	1316
Total Number of Staff	1200
Facilities	64
AUB campus size (m²)	259,000

This conducted demand-side research survey on shared micro-mobility at AUB university campus tends to focus on questions such as how and why this specific service might be used by the community. Thus, this survey can be further classified by distinct factors that influence the service demand. The first factor includes user socio-demographic aspects such as gender, status, age group, and the faculty enrolled in or

work at AUB. The second factor involves service attributes such as the safety measures (scooters lanes and speed limit), network coverage (stations locations), and e-scooter service time window. Yet, the most vital factor that has a direct impact on formulating the demand is the e-scooter trip-related issues which encompass user's origins/destinations and the time of use of e-scooter per day and per week. The latter factor conveys each user's most frequent commuting patterns and thus his/her distance traveled by measuring the kilometers between each origin and destination station. Also, by specifying the time intervals that the user will most probably use the e-scooter service in during both weekends and weekdays (morning peak interval, midday interval, peak afternoon interval, evening interval), an e-scooter hourly transportation demand can be thus computed. Figure 7 shows a typical weekday hourly e-scooter demand. It can be noticed that the number of trips fluctuates during the day and reaches a peak of 60 trips at 8:00 a.m. and 4 p.m. before falling again. However, the survey reveals that 10% of the respondents attempt to use e-scooters during weekends.

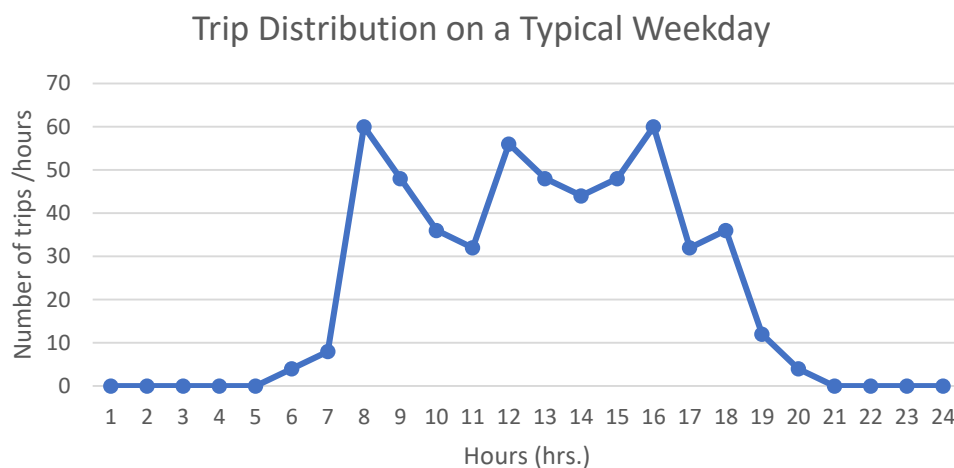


Figure 7: Typical weekday hourly e-scooter transportation demand.

Moreover, provided the heterogeneity of the e-scooter commuting system at each station, the statistical analysis showed 50 distinct commuting patterns among the

13 stations. This origin/destination data per trip give valuable performance measures such as trip length that is the distance covered by the user per trip and the most popular origin/destination pairs. To clarify, suppose a student usually enters AUB from AUB main gate and goes to the BECHTEL building to attend his/her lectures. His/her commuting pattern will be as follow: origin is AUB main gate station, the destination is BECHTEL station (C-ENG) and hence the distance covered for such a pattern is 0.55 km. With this in mind, each trip pattern can then be considered in kilometers and thus the hourly transportation demand profile of a typical weekend/weekday expressed in kilometers is shown in Figure 8.

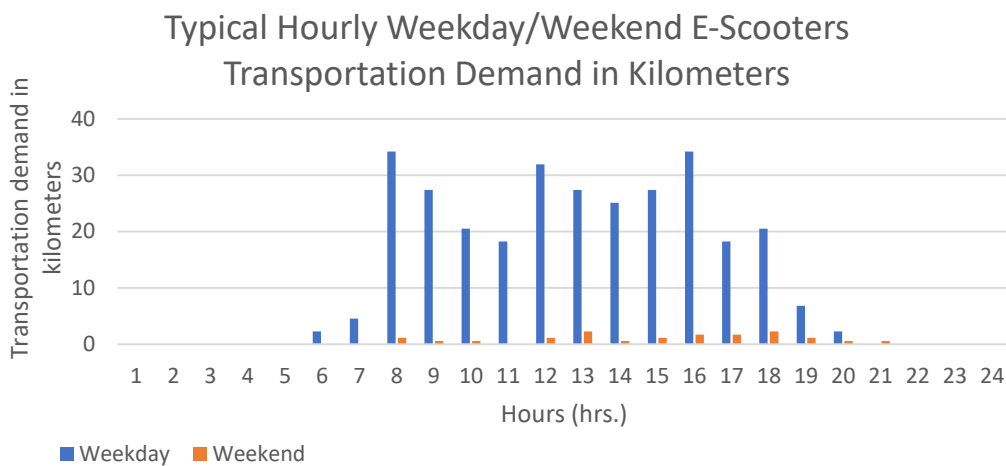


Figure 8: Hourly e-scooter transportation demand for a typical weekday/weekend expressed in kilometers.

The e-scooter is regarded as a dynamic storage system and as such, the obtained hourly kilometer demand is then converted to an hourly kWh demand, given that the e-scooter requires 9.14 watt-hour energy per kilometer.

However, as the magnitude of the factors affecting the service demand varies with respect to the time of the day and the time of the week, it does also vary according to the month of the year. This is due to adverse weather conditions and the variation of the number of students, staff, and employees available on campus. So to account for such

variations, a semester-based typical year demand is formulated such that the obtained typical weekday/weekend profile is multiplied by 120%, 130%, 50%, and 10% to correspond to the Fall, Spring, Summer and August semesters, respectively. Therefore, the resulting transportation demand accounting for hourly, daily, and seasonal variations is described in Figure 9. An extra energy percentage was added to the forecasted demand for the sake of the respondent's and AUB population's unexpected daily additional trips.

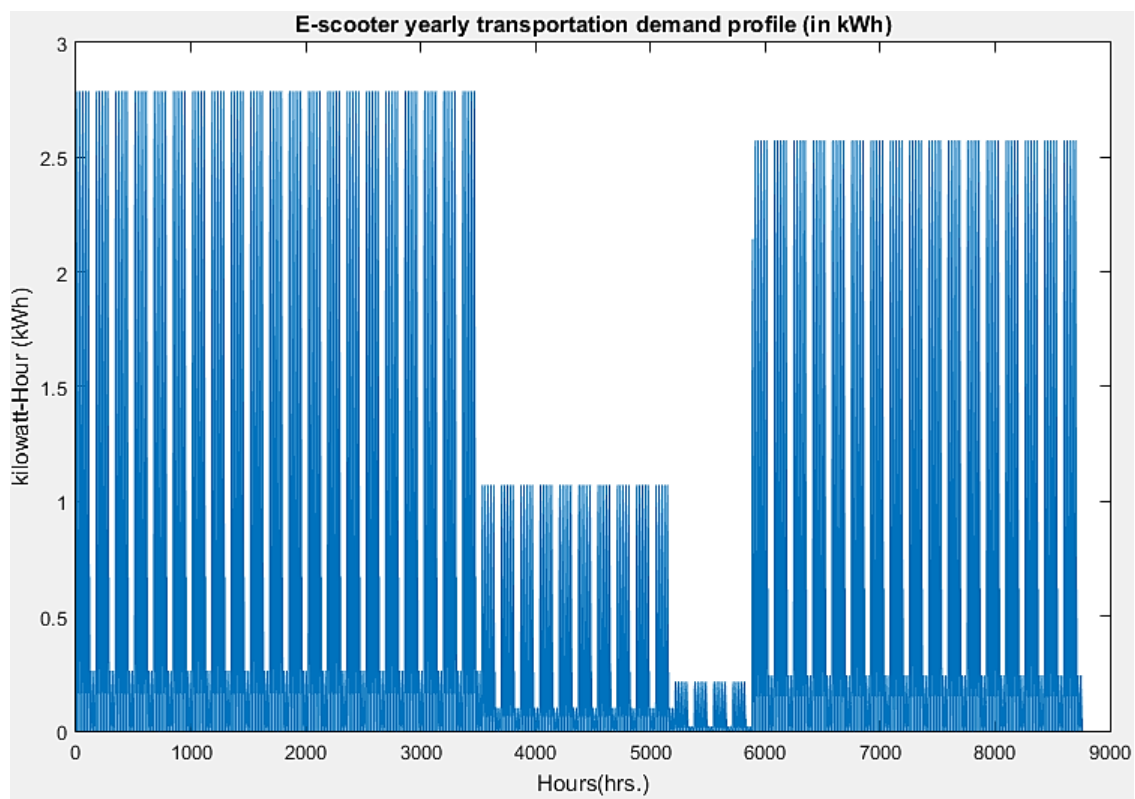


Figure 9: E-scooter's yearly transportation demand expressed in kilowatt-hour considering seasonal, daily and hourly variations for the sample population considered.

As a matter of fact, this formulated e-scooter transportation demand is derived based on user global satisfaction factors including trip duration, service accessibility, network connectivity, comfort and safety issues without taking into consideration the charge rate in \$/kilometer. By all means, this cost is a fundamental element because it can possess a radical direct effect on increasing or decreasing the demand for such a

service. With this in mind, the attractiveness of this project and the willingness of the AUB community to use the e-scooters are directly proportional to the cost assigned to each trip. For instance, a high charging cost on each trip will decrease the attractiveness and willingness of users to satisfy their transportation demand via this service. On the other hand, if the charging cost was relatively low, the user's willingness to use an e-scooter to satisfy their transportation will increase.

Accordingly, the above formulated transportation demand is considered to be the full transportation demand that corresponds to the expected number of students and faculty to request e-scooters at a certain time "t". In reality, this full demand should be modified so that global user satisfaction includes the cost of using this service. For this reason, a second quantity is computed that represents the actual hourly transportation demand, which tells the actual demand supplied by e-scooters during that time "t" taking into account this cost factor. Consequently, the actual transportation demand at any instant will range between 0 and the full transportation demand observed at that instant, where zero illustrates that none of the transportation demand at time a "t" is supplied by e-scooters.

This is accomplished by formulating a cost-attractiveness function that relates the full transportation demand to the actual transportation demand. This function is computed by asking users in the conducted survey to specify the expected minimum and maximum cost that they are willing to pay per kilometer. These values determine the range of the function (0 to 4\$). Next, the user should rate each of the three suggested costs: 1.32 \$/km, 1.65 \$/km, and 2 \$/km. These ratings convey how much the user is willing to pay for using such a service. Afterward, the average values of the satisfaction indices associated with different ranges of costs are calculated based on the collected

ratings. These nine quantities are represented by the blue circles in Figure 10. Finally, a generalized linear regression model (GLM) is then used to fit the average satisfaction indices and their associated costs as shown in Figure 10. The dependent variable in this model follows a binomial distribution whose logit differs linearly with the independent variable [37]. The curve reveals the cost-attractiveness function desired which specifies the total satisfaction index of the users at a given cost. It is clear that the charge rate per kilometer decreases as the user's satisfaction index increases and vice versa.

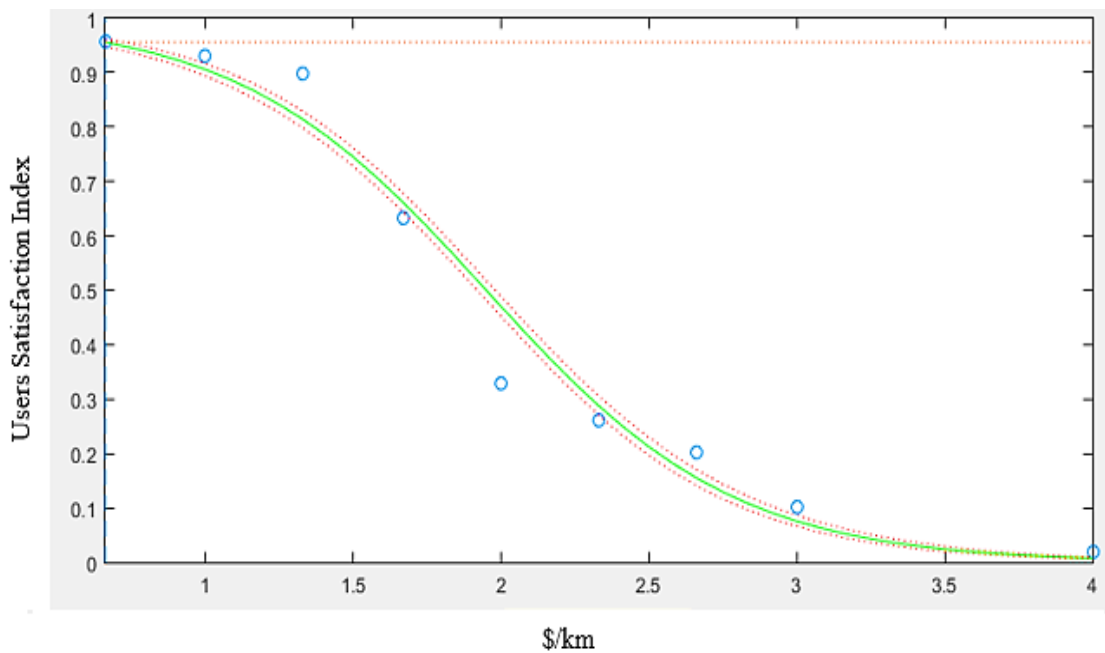


Figure 10: Users satisfaction index as a function of the charge cost per kilometer.

CHAPTER 5

METHODOLOGY

This research proposes a methodology to redesign the power supply of a MG characterized by scheduled blackouts and heavy reliance on diesel generators. The new design seeks a solution beyond diesel generators by combining clean energy resources such as PV system and BSS. In addition to that, EVs are considered as a substitute for conventional fuel-based vehicles used for work-related trips. This work also studies the feasibility of integrating an e-scooter sharing system. These transportation services (EVs and e-scooters) also play a secondary role by acting as a battery storage system after reserving the energy required to fulfill their transportation demand. Thus, to examine such a system two main optimization stages are implemented and discussed in sections 5.1 and 5.2, respectively.

The first optimization level aims to converge to the optimal capacity of the PV-BSS hybrid system along with finding the optimal charge rate (\$/km) to be imposed on using the e-scooters while ensuring an efficient reliable secured source of energy, diminishing carbon footprint through reducing diesel dependency, and reducing the total cost of the MG in terms of operation and investment. Owing to the nonlinear and non-convex nature of this capacity planning problem, this sizing optimization stage is implemented via local minimization optimization techniques and is assisted by a non-optimal rule-based EMS that aims to manage the power flow from the dispatchable resources. This rule-based algorithm is based on prior knowledge and experience of the system to build a set of rules for an efficient yet non-optimal interaction between the available energy resources and demand. The advantage of using a rule-based EMS in

this sizing optimization level is being computationally highly efficient while considering the hourly entire year data that include the varying weather, electrical, and transportation demand conditions.

The second optimization level aims to find the optimal performance of the configured MG by optimally optimizing its operation under an optimal EMS. This is achieved by minimizing the daily operational cost of the entire MG using convex optimization technique.

5.1. First Optimization Level:

This level is a multi-objective optimization problem formulated to converge to the optimal sizes of the power system resources (PV-BSS) along with finding the charge rate per kilometer (\$/km) which is to be imposed on using e-scooters, so that the project remains within its feasible boundaries. For this purpose, the objective of such optimization is to minimize the annual operating cost of the MG which is illustrated in the following equation:

$$F = f_1 - f_2 + f_3 \quad (30)$$

(f_1) aims to minimize AUB carbon footprint by reducing the carbon emissions produced on campus. Those emissions can be classified into direct and indirect ones. Emissions that are due to fuel burned in onsite electricity generators and that are produced from transport vehicles owned by the university are regarded as direct emissions. While the indirect emissions include emissions from electricity consumption required for supplying university load demand through EDL. Therefore, f_1 is formulated as follow [82]:

$$f_1 = (E_{Grid} + E_{Die}) * \alpha \quad (31)$$

$$E_{Grid} = \sum_{t=1}^{8760} P^{EDL}(t) * K_{CO_2-Grid} \quad (32)$$

$$E_{Die} = EFF * \sum_{t=1}^{8760} P^{Die}(t) * L_{kWh} * NCV * D * 10^{-6} \quad (33)$$

where, E_{Grid} and E_{Die} are the annual carbon emissions due to utility grid's purchased energy and diesel generator energy in kg, respectively. α represents the tax on carbon emissions in \$/kg. It is important to note that, emissions due to conventional vehicles in the new system is not considered as they are replaced by electrical ones. $P^{EDL}(t)$ and $P^{Die}(t)$ are the grid's purchased active power and diesel's generator output power in kW, respectively. K_{CO_2-Grid} is the grid's carbon footprint in kg/kWh, EFF represents the emissions factor of fuel (diesel) in tons of CO₂-e/TJ, L_{kwh} is the fuel consumption per kilo-watt hour of electricity in L/kWh, NCV is the net calorific value of diesel in TJ/Gg, and D is the density of diesel in kg/L.

This optimization also considers maximizing revenues from the integration of EVs and e-scooters project using (f_2). This revenue is illustrated by the amount of money paid by students, faculty, and staff who use the e-scooter service. It is expressed by (r), and it is mainly influenced by two factors: the first one is the charge rate per kilometer and the second one is the global satisfaction related to the service attributes. The savings resulting from discharging the EVs and e-scooters during peak tariff hours are shown in low energy consumption from EDL. Thus, the following set of equations model (f_2):

$$f_2 = r - (CC^{SC} * CRF^{SC} + CC^{EV} * CRF^{EV} + OM^{SC} + CF_{charging}) \quad (34)$$

$$r = \sum_{t=1}^{8760} C * U(C) \quad (35)$$

$$U(C) = \frac{e^{4.6449-0.0016*C}}{1 + e^{4.6449-0.0016*C}} * FT \quad (36)$$

$$CF_{charging} = \left(\sum_{t=1}^{8760} P_{ch,EDL}^{EV}(t) + \sum_{t=1}^{8760} P_{ch,EDL}^{SC}(t) \right) \times EDL_{Tariff}(t) \quad (37)$$

where, r is the annual revenue gained from charges imposed on e-scooter trips in \$ and $CF_{charging}$ is the e-scooters and EVs annual charging cost in \$. C is the charge rate of using an e-scooter in \$/km, $U(C)$ is the cost-attractiveness function, and FT is the full transportation demand in km/hr.

The last goal targeted in this optimization level is the annual operating cost of the MG's distributed resources (excluding EVs and e-scooters). Annual operation cost is a minimization problem illustrated by the following equation:

$$f_3 = \sum_{t=1}^{8760} (P^{EDL}(t) * EDL_{Tariff}(t)) + (P^{PV}(t) * COE^{PV}) + (P^{Die}(t) * COE^{Die}) + (P_{dch}^{BSS}(t) * COE^{BSS}) \quad (38)$$

5.1.1 Proposed Rule-Based Energy Management System:

The intermittent nature of power generation from EDL and PV systems is the reason behind using BSS and diesel generators as a backup source of energy. Thus, the need to implement an EMS to balance between demand and generation is crucial. The EMS main goal however, is to coordinate and economically manage the power coming from the MG energy sources while ensuring the full utilization of the PV system and the reduction of diesel generators dependency. Besides, this control approach plays a vital role in managing the BSS, EVs and e-scooters since they are considered to be dispatchable sources. Thus, their COE is strongly affected by their dispatch strategies,

and specifically, the COE^{BSS} which is influenced by the BSS installed capacity as well. The EMS implemented in this level is designed and applied using a rule-based algorithm which is made to run on hourly basis for an entire year period to capture all input variations (PV output variations), electric demand variations, and the transportation demand variations. This conditional algorithm is basically in the form of ‘if’ then ‘else’ statements which are related to several scenarios that execute the operating mode associated to each one. Each mode then permits the energy flow from different resources available in the MG according to specific pre-defined rules. The major scenarios are defined based on the grid’s ON/OFF states and peak tariff hours’ occurrence as illustrated in Figure 11.

The implemented algorithm first computes the energy generated by the PV system based on the measured climatological conditions and the initial value of the SOC specified. Then, the rule based algorithm utilizes this data to reduce diesel dependency and grid’s peak tariff purchased energy to its greatest extent while charging the BSS, EVs, and e-scooters during night tariffs hours only. So as it can be interpreted from Figure 11, that the rule-based EMS starts by checking if EDL is ON or OFF:

- If OFF, it will determine to what time interval this time slot belongs:
 - _ If it belongs to day-time interval ($7 a. m. \leq t < 4 p. m.$) then the PV system, the BSS and the forecasted excess energy from e-scooters batteries during that day are used to supply the electrical demand.
 - _ If this hourly time slot occurs during peak demand hours ($4 p. m. \leq t < 11 p. m.$) then the PV system, the BSS and the forecasted excess energy from e-scooters and EVs batteries during that day are used to supply load.

- _ Otherwise it will correspond to the interval $11 p.m. \leq t < 7 a.m.$ and therefore the BSS only will be responsible for supplying load.

It's crucial to highlight that the diesel generators remain acting as the primary backup source of energy in this case. That is, if any generation deficiency from the clean energy resources happened at any time slot during a grid's outage it will be supported by diesel generators. However, the reliance on such a polluting source will be minimized.

- If EDL was ON, the EMS will check whether this time slot corresponds to a peak tariff interval or not.:
 - _ If it corresponds to a peak tariff hour, it will check whether a blackout occurs during that day or not. If a blackout occurs, then the algorithm will aim to minimize the grid's peak tariff purchased energy by supplying load via PV system, BSS, e-scooters and EVs left-over energy. Otherwise, it will use EDL.
 - _ If it corresponds to off peak hours, the algorithm will supply the demand from the PV system and grid only and charge the BSS, EVs, and e-scooters batteries during night tariff hours.

Thereby, the utility grid will be satisfying the gap between PV generation and electrical demand whenever available.

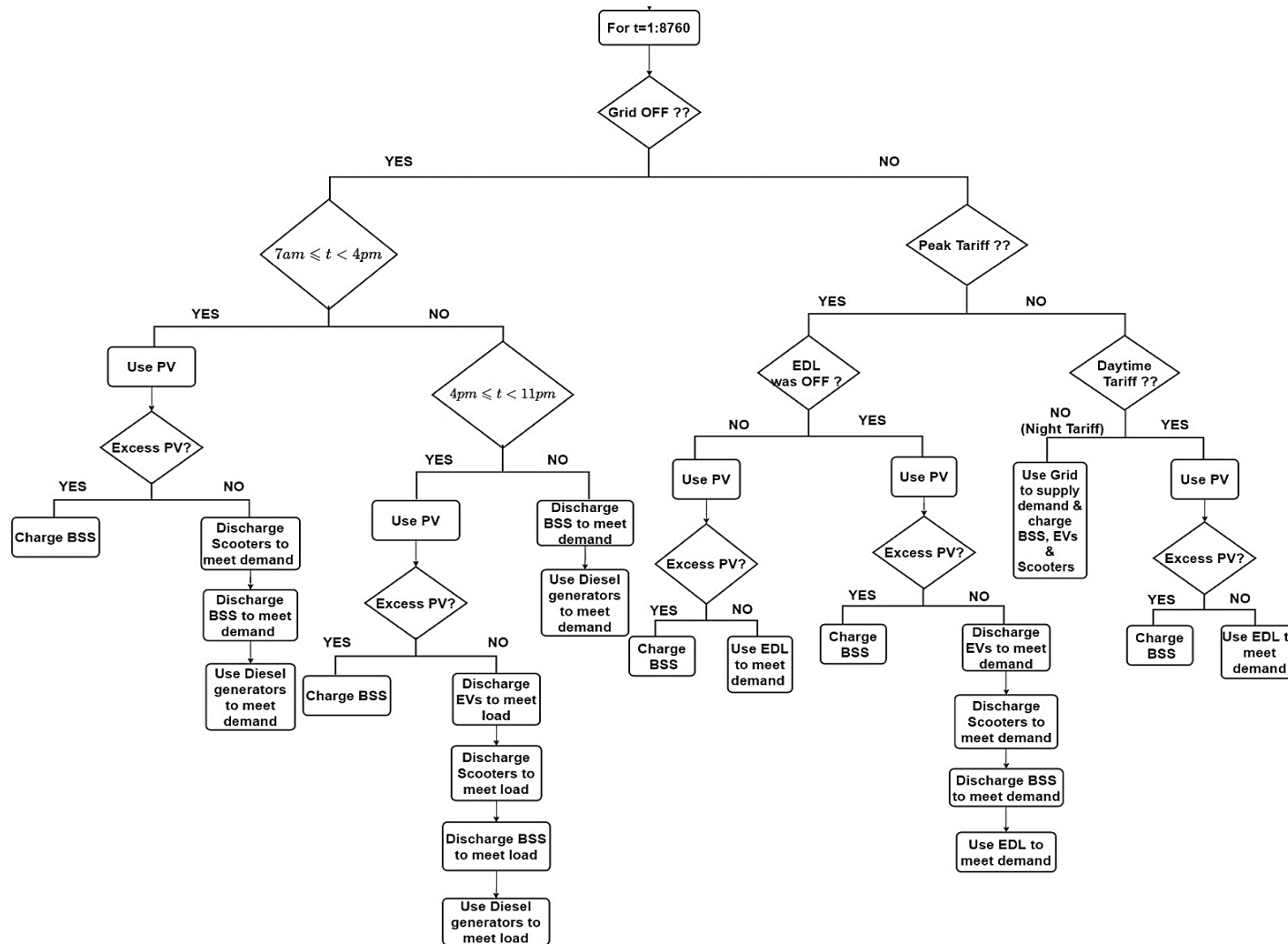


Figure 11: Rule-Based EMS

5.1.2. Proposed Optimization Techniques:

The optimization problem described next considers the PV system capacity, BSS capacity and e-scooters charge rate per km (\$/km) as the design variables. The optimization problem is then formulated by minimizing F subject to the upper and lower bounds of the decision variables as follow:

$$\mathbf{min} F$$

$$\mathbf{Subject\ to} \quad 0 \leq PV_{capacity} \leq 2400 \text{ kW} \quad (39)$$

$$0 \leq BSS_{capacity} \leq 9000 \text{ kW} \quad (40)$$

$$1 \text{ \$/km} \leq x \leq 4 \text{ \$/km} \quad (41)$$

Owing to the non-linearity and non-convexity of this sizing and planning problem, the proposed rule-based EMS is being optimized by the use of local minimization techniques.

5.1.2.1 Method One: Particle Swarm Optimization:

Particle swarm optimization (PSO) is one of the most well-known metaheuristic techniques; inspired by the motion of bird flocks and schooling fish. The PSO algorithm works by having a population (named as swarm) of candidate solutions (called particles). It starts with a random group of particles/solutions in the design space. These solutions are identified by two vectors the position vector (χ_i) and the velocity vector (v_i). The movement of these particles in the search-space is directed by their own best-known position (B_i) in the search-space as well as the entire swarm's best-known position (P_i), this is accomplished according to the following equations:

$$v_i(t + 1) = \phi v_i(t) + \alpha_1[\beta_1, B_i(t) - \chi_i(t)] + \alpha_2[\beta_2, P_i(t) - \chi_i(t)] \quad (42)$$

$$\chi_i(t + 1) = \chi_i(t) + v_i(t + 1) \quad (43)$$

where $v_i(t)$ and $x_i(t)$ are the current velocity and position of particle i in the swarm, respectively. ϕ is the particle inertia which gives rise to a certain momentum of the particles. β_1, β_2 are uniformly distributed random values while α_1, α_2 are the acceleration constants. The movement of the swarm occurs when improved positions are being revealed, and this process is repeated until a satisfactory solution is attained [83]. PSO algorithm is described in Figure 12. The stopping criterion can be the number of iterations, the convergence of the swarm, or the attainment of a specific goal fitness value. The PSO built in function in MATLAB environment has been utilized to find the optimal decision variables [84]. A swarm size of 100 particles was considered. The PSO algorithm is set to iterates until the relative change in the best objective function value over the last 20 iterations is less than e^{-6} .

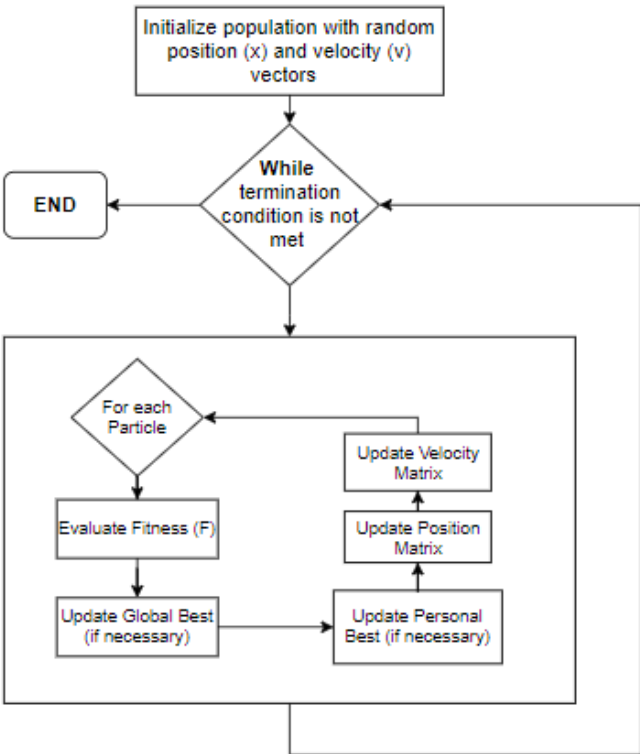


Figure 12: Particle swarm optimization flow chart [85].

5.1.2.2. Method Two: FMINCON Solver vis Yalmip Parser

A second method was applied to solve this non-convex non-linear optimization problem. As a matter of fact, the convexity of the objective function can be attained by restricting the range of the user attractiveness function to 2.23\$/km instead of 4\$/km. However, the non-convexity and non-linearity presented are due to the presence of non-linear constraints in the ‘if’ then ‘else’ rule-based algorithm. Thus, the use of a non-linear solver is needed. This is referred to as non-linear programming. To this end, FMINCON solver is utilized via YALMIP optimization toolbox in Matlab environment [86] and is used to optimize the rule-based EMS to compute the decision variables. FMINCON solver implements the interior point method (IPM) algorithm [87]. This algorithm tries to solve a constrained minimization problem by treating it as a sequence of approximated minimization problems starting at an initial estimate [88].

By combining either PSO or FMINCON with the rule-based EMS, this sizing planning optimization approach will converge to the system’s optimization variables that achieve a minimum annual system’s cost. These implemented local minimization optimization techniques are simple yet the quality of their solution is very sensitive to solver initializations. Depending on each initialization, those techniques can converge to distinct local minima more or less close to the optimal solution. To overpass those restrictions and improve significantly the efficiency of local minimization techniques applied, grids that represent multiple initialization points are implemented to each methodology. This has been illustrated in Figures 13 and 14. It is worth noting that random initializations were also taken into consideration and are symbolized by the red stars. The real value of this structured grid is that starting from any of these initial

points in the search space, the optimization techniques used converge to the same solution. Consequently, this local minimum can be regarded as the optimal solution.

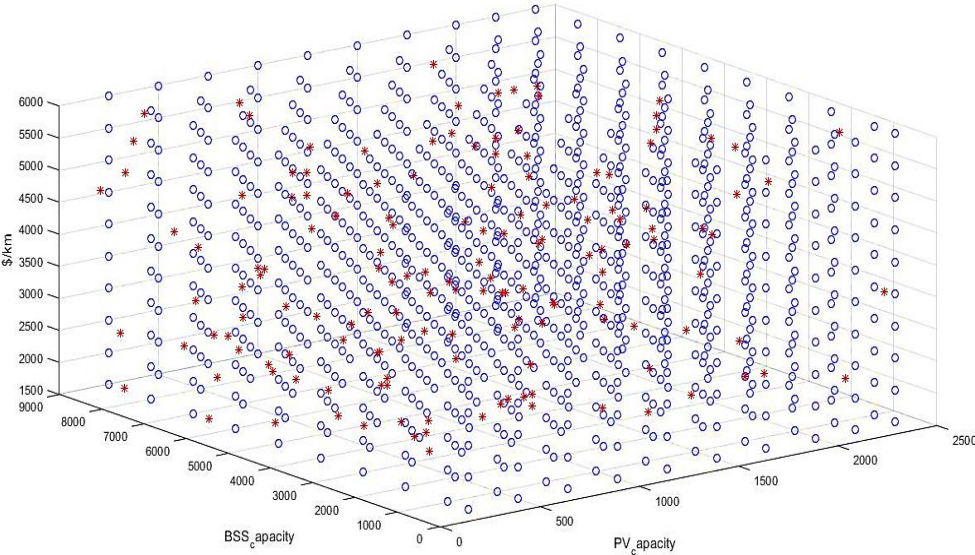


Figure 13: FMINCON solver multi-initialization grid in terms of PV capacity, BSS capacity, and \$/km. Blue stars represent distinct structured initializations while the red ones represent random initialization in the search space. In total, the simulation was performed for 1150 initial points.

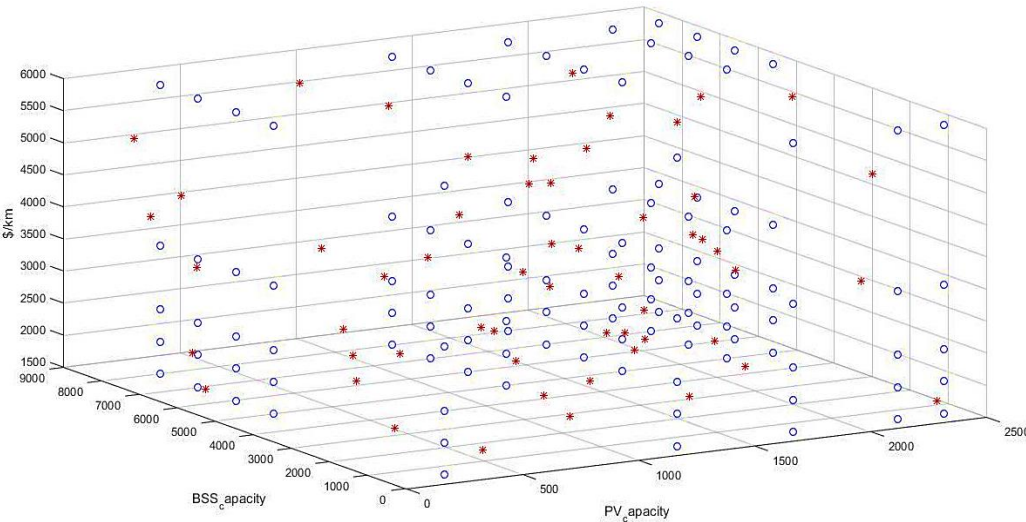


Figure 14: Particle Swarm Optimization multi-initialization grid as a function of PV capacity, BSS capacity, and \$/km. Blue stars represent distinct structured initializations while red one represent random initialization in the search space. In total, simulations was performed considering 170 initial point.

Although both PSO and FMINCON are regarded as nonlinear minimization solvers, however, FMINCON presents a number of benefits over PSO. These advantages are in terms of very short simulation time, fewer number of iterations to solve, non-dependency on population size and value, applicable to different sizes of problems, thereby rendering it more efficient. This has been proven by recording the time of 10 simulations starting from different initializations in each method. The results showed that PSO spends an average of 160 min per 10 simulations whereas, the FMINCON solver utilized in the YALMIP optimization toolbox spends an average of 20 min per 10 simulations. As a result, the FMINCON initialization grid is denser and thus more efficient and robust to the obtained solution than that of the PSO. All simulations were performed using MATLAB software on an Intel Core i7-4510U CPU, 2.00GHz, 2601 MHz PC.

5.2. Second Optimization Level:

The second stage deals with finding the optimal dispatch profile of the MG configuration obtained. This is achieved by minimizing the daily operational cost of the entire MG using a weighted objective function that is illustrated in the following equation:

$$\begin{aligned} \min J = \sum_{t=1}^{24} [& (P^{EDL}(t) * EDL_{Tariff}(t))\delta_1 + (P^{PV}(t) * COE^{PV})\delta_2 + \\ & (P^{Die}(t) * COE^{Die})\delta_3 + (P_{dch}^{EV}(t) * COE^{EV})\delta_4 + \\ & (P_{dch}^{SC}(t) * COE^{SC})\delta_5 + (P_{dch}^{BSS}(t) * COE^{BSS})\delta_6] \end{aligned} \quad (44)$$

where, $\delta_1, \delta_2, \delta_3, \delta_4, \delta_5$ and δ_6 are the weights assigned on grid's, PV, diesel, EV, scooter, and BSS output power, respectively. Considering the grid's triple tariff rate

scheme, the weights assigned to each energy source are depicted in Table 15, will lead to the following energy dispatching profile:

- No penalty will be assigned on PV output energy.
- Diesel generator is the most penalized source of energy.
- BSS's ultimate goal is to reduce diesel dependency and grids' peak purchased energy after having to replace diesel generator's energy.
- Available EVs and e-scooters can also help in reducing diesel generator energy or grid's peak purchased energy after fulfilling their transportation demand.

Table 13: Weights assigned to the MGs energy sources.	
Weights	Values
δ_1	20
δ_2	1
δ_3	50
δ_4	7.3
δ_5	1
δ_6	15

5.2.1. Proposed Optimization Technique:

The MG planning problem is inherently a non-convex and a non-linear problem due to the presence of binary variables. These variables are used to represent the ON/OFF state of each dispatchable source. However, those integer variables need to be determined prior to the convex optimization to preserve convexity. Particularly, for convexity to exist the following conditions must be met:

- _ The objective function J must be convex.
- _ The inequality functions must be convex.
- _ The equality functions must be affine.

Therefore, the decision criterion on power resources ON/OFF profiles and the computation of e-scooters and EVs excess energy is determined at the beginning of each day of the year prior to the optimization stage according to the following set of rules:

- Diesel generators are allowed to supply load demand when EDL is OFF. Thus, the diesel ON/OFF profile is expressed by the following expression:

$$\lambda(t) = 1 - EDL_{profile}(t) \quad (45)$$

where $EDL_{profile}(t)$ is a binary decision variable that represents the grid state (ON/OFF) at time t .

- Charging of the BSS, EVs, and e-scooters is allowed only when EDL is ON and EDL is at night tariff hours. Thus, the charging profile $x(t)$ is illustrated by the following expression:

$$x(t) = EDL_{night} * EDL_{profile}(t) \quad (46)$$

where, EDL_{night} represents the profile of night tariff hours.

- Discharging of BSS and e-scooters excess energy are allowed during EDL outage hours and EDL peak tariff hours if the outage of that day has already occurred. This is expressed by the following discharging profile:

$$y(t) = j * EDL_{peak} + (1 - EDL_{profile}(t)) \quad (47)$$

where, EDL_{peak} represents the profile of the peak tariff hours, and j is a flag variable that goes to 1 if an outage has already occurred and 0 otherwise.

- Discharging of EVs is permitted at the end of AUB personnel working hours (from 4:00 pm to 11:00 pm) if an EDL outage has already occurred. This is clearly described by the following expression:

$$y_{ev}(t) = j * EDL_{afternoon}(t) \quad (48)$$

where, $EDL_{afternoon}$ is the EDL profile starting from peak tariff hours.

Secondly, the non-linearities of the problem are removed by linearizing the multiplications of binary profiles and the continuous variables.

Accordingly, the resulting convex optimization problem is described by the following convex objective function and constraints and the affine equalities:

min J

$$\text{Subject to } P^{BSS}(t) - P_{dch}^{BSS}(t) + P_{ch}^{BSS}(t) = 0 \quad (49)$$

$$0 - P_{ch}^{BSS}(t) \leq 0 \quad (50)$$

$$P_{ch}^{BSS}(t) - P_{ch,max}^{BSS} * x(t) \leq 0 \quad (51)$$

$$0 - P_{dch}^{BSS}(t) \leq 0 \quad (52)$$

$$P_{dch}^{BSS}(t) - P_{dch,max}^{BSS} * y(t) \leq 0 \quad (53)$$

$$SOE_{min}^{BSS} - SOE^{BSS}(t) \leq 0 \quad (54)$$

$$SOE^{BSS}(t) - SOE_{max}^{BSS} \leq 0 \quad (55)$$

$$SOE^{BSS}(t) = SOE^{BSS}(t-1) - P_{dch}^{BSS}(t) + P_{ch}^{BSS}(t) * \eta^{BSS} \quad (56)$$

$$P^{SC}(t) - P_{dch}^{SC}(t) + P_{ch}^{SC}(t) = 0 \quad (57)$$

$$0 - P_{ch}^{SC}(t) \leq 0 \quad (58)$$

$$P_{ch}^{SC}(t) - P_{ch,max}^{SC} * x(t) \leq 0 \quad (59)$$

$$0 - P_{dch}^{SC}(t) \leq 0 \quad (60)$$

$$P_{dch}^{SC}(t) - P_{dch,max}^{SC} * y(t) \leq 0 \quad (61)$$

$$SOE_{min}^{SC} - SOE^{SC}(t) \leq 0 \quad (62)$$

$$SOE^{SC}(t) - SOE_{max}^{SC} \leq 0 \quad (63)$$

$$SOE^{SC}(t) = SOE^{SC}(t-1) - P_{dch}^{SC}(t) + P_{ch}^{SC}(t) * \eta^{SC} \quad (64)$$

$$P^{EV}(t) - P_{dch}^{EV}(t) + P_{ch}^{EV}(t) = 0 \quad (65)$$

$$0 - P_{ch}^{EV}(t) \leq 0 \quad (66)$$

$$P_{ch}^{EV}(t) - P_{ch,max}^{EV} * x(t) \leq 0 \quad (67)$$

$$0 - P_{dch}^{EV}(t) \leq 0 \quad (68)$$

$$P_{dch}^{EV}(t) - P_{dch,max}^{EV} * y_{ev}(t) \leq 0 \quad (69)$$

$$SOE_{min}^{EV} - SOE^{EV}(t) \leq 0 \quad (70)$$

$$SOE^{EV}(t) - SOE_{max}^{EV} \leq 0 \quad (71)$$

$$SOE^{EV}(t) = SOE^{EV}(t-1) - P_{dch}^{EV}(t) + P_{ch}^{EV}(t) * \eta^{EV} \quad (72)$$

$$0 - P^{Die}(t) \leq 0 \quad (73)$$

$$P^{Die}(t) - P_{max}^{Die} * \lambda(t) \leq 0 \quad (74)$$

$$0 - P^{EDL}(t) \leq 0 \quad (75)$$

$$P^{EDL}(t) - P_{max}^{EDL} * EDL_{profile}(t) \leq 0 \quad (76)$$

$$p^{demand}(t) - P^{Die}(t) - P^{EDL}(t) - P^{PV}(t) - P_{dch}^{SC}(t) * \eta^{SC} - P_{dch}^{BSS}(t) * \eta^{BSS} - P_{dch}^{EV}(t) * \eta^{EV} + P_{ch}^{SC}(t) + P_{ch}^{EV}(t) + P_{ch}^{BSS}(t) = 0 \quad (77)$$

Constraints (49), (57), and (65) enforces the BSS, e-scooters batteries, and EVs batteries to be in only one of the charging and discharging states at each time slot t. Constraints (50 – 53), (58 – 61), and (66 – 69) show the range of charge and discharge of the BSS, e-scooters batteries, and EVs batteries at each time slot t, respectively. Constraints (54 – 55), (62 – 63), and (70 – 71) show the range of the state of energy of the BSS, e-scooters batteries, and EVs batteries at each time slot t. Constraints (56), (64), and (72) represent the stored energy in the BSS, e-scooters batteries, and EVs batteries at each time slot t, respectively. Constraints (73 – 76) represent the output generation limits of the diesel generator and grid. Constraint (77) is the load balance constraint that ensures that each time slot t the power generated from all sources meets demand. These equality and non-equality constraints of the problem in hand are linear,

hence the feasible set of the given problem is also convex. This convex method adopted is a mathematical method that yields to a global optimal solution, thus CVX Toolbox is used. CVX is a high-level powerful MATLAB-based modeling tool for disciplined convex programming optimization [89]. CVX supports numerous standard problem types, involving linear and quadratic programs (LPs/QPs), second order cone programs (SOCPs) and semidefinite programs (SDPs). CVX is able to solve more sophisticated convex optimization problems that include non-differentiable functions.

CHAPTER 6

RESULTS

This chapter presents the validity of the contributions introduced in this research within the context of developing an optimal capacity planning approach of a microgrid characterized by scheduled blackout. The reduction of diesel generators dependency during grid's outages is well achieved in presence of the clean energy resources PV and BSS systems. These sources are optimally sized in the first stage optimization approach coupled with the consideration of EVs as a substitute for conventional fuel-based vehicles used for work-related trips. Also, the project of integrating an e-scooter sharing system to help AUB community commute easily within campus is considered feasible as it recorded significant revenues. These transportation services (EVs and e-scooters) also play a secondary role by acting as a battery storage system after reserving the energy required to fulfill their transportation demand. After obtaining the optimally configuration of the microgrid, the optimal planning of such a microgrid was achieved by running the system under an optimal EMS.

The outcomes resulting from the developed capacity rule-based planning optimization stage is detailed in section 6.1. Followed by the results of the optimal planning optimization stage in section 6.2. This chapter also presents a sensitivity analysis conducted in section 6.3 to illustrate the different economic viewpoints of the proposed optimal MG planning approach.

6.1. First Level optimization

In this optimization level, FMINCON via Yalmip parser and PSO result in the same optimal PV capacity (2400 kW), BSS capacity (6330 kW), and charge rate per kilometer (1.51 \$/km). However as discussed earlier, PSO is much more computationally demanding in comparison to FMINCON via Yalmip parser. The technical and economic input specifications of MG sources along with the optimization results are depicted in tables 14 and 15, respectively.

The number of e-scooters to be integrated into the sharing system is 500 and it was selected based on the space available on campus to install the e-scooter stations and the actual transportation demand that these e-scooters have to satisfy. It's critical to note that the revenues attained from the integration of the e-scooter sharing system reach 544,511\$. This result has further strengthened the confidence in investing in this sharing system on AUB campus as an integral, reliable, and profitable commuting system that will aid AUB community to satisfy their first-mile-last-mile travel.

Table 14: Technical and economic input specifications of the MG components.

Parameters	Values	Units
Project life	12	years
Inverters Efficiency	95	%
PV Capital Cost	2,098,320	\$
PV Operation and Maintenance Cost	21,144	\$/year
PV Loan Interest Rate	5	%
PV Loan Period	10	years
PV Loan Annual Payment	292,866	\$
BSS Capital Cost	7,766,910	\$
BSS Operation and Maintenance Cost	25,985	\$/year
BSS Loan Interest Rate	5	%
BSS Loan Period	10	years
BSS Loan Annual Payment	1,031,835	\$
EVs Capital Cost	1,675,585	\$

EVs Loan Interest Rate	5	%
EVs Loan Period	10	years
EVs Loan Annual Payment	216,996	\$
E-scooter Quantity	500	units
E-scooter Total Storage	288	kWh
E-scooters Capital Cost	392,500	\$
E-Scooter Operation and Maintenance Cost	75,000	\$/year
E-scooter Loan Interest Rate	5	%
E-scooter Loan Period and Project Life	3	years
E-scooter Loan Annual Payment	219,129	\$
Diesel Generators Operation and Maintenance Cost	20,298	\$
Diesel Generator Fuel Cost	1.04	\$/L
Diesel Fuel Density	0.8439	Kg/L
Diesel Emission Factor (EFF)	74,100	Kg CO ₂ -e/TJ
Diesel Consumption Factor	0.275	L/kWh
Diesel Net Colorific Value (NCV)	43	TJ/Gg
EDL Daytime Tariff Rate	0.073	\$/kWh
EDL Night Tariff Rate	0.05	\$/kWh
EDL Peak Tariff Rate	0.213	\$/kWh
Grid's Carbon Emission Factor	0.75	kg/kWh
Tax on Carbon Emissions	0.02	\$/kg

Table 15: First stage optimization results.

Decision Variables	Values	Units
Optimal PV capacity	2,400	kW
Optimal BSS capacity	6,330	kW
E-scooter Optimal Charge rate per kilometer	1.51	\$/km

6.2. Second Optimization Results

The second stage decision variables are the operating variables that determine the amount of power that needs to be generated from each source such that the daily operational cost is minimized by the formulated weighted objective function. At the beginning of each day, the EVs and e-scooter's maximum state of energy are calculated

based on the required energy to be reserved for the transportation demand on that particular day.

The resulted annual energy profile for the proposed system in comparison to the original one is illustrated in the following table:

	Existing Power System	Proposed Power System
Annual Grid's Energy (kWh)	30,208,624	42,134,462
Annual Diesel's Energy (kWh)	16,335,326	693,301
Annual EVs Disch. Energy (kWh)	-	656,987
Annual E-scooters Disch. Energy (kWh)	-	85,677
Annual BSS Disch. Energy (kWh)	-	5,971,324
Annual PV Energy (kWh)	-	4,441,521
Load (kWh)	46,543,950	46,543,950
Total Generation (kWh)	46,543,950	53,983,272
Demand (kWh)	46,543,950	53,983,272
DG share (%)	35	1.28
Clean Energy share (%)	-	20.66
Grid's Cost (\$)	2,953,308	3,571,773
Diesel's Cost (\$)	4,900,598	207,990
BSS's Annual Payment (\$)	-	1,031,835
PV's Annual Payment (\$)	-	292,886
EVs 's Annual Payment (\$)	-	216,996
E-scooter's Annual Payment (\$)	-	219,129
E-scooter's Revenues (\$)	-	544,511
Fuel Cost for Vehicles (\$)	93,128	19,493
EVs Cost of Charging (\$)	-	38,582
E-scooters Cost of Charging (\$)	-	5,031
BSS Cost of Charging (\$)	-	350,671
Total Cost (\$)	7,947,034	5,015,592
Cost of Energy (\$/kWh)	0.169	0.093
Savings (\$)		2,931,442

These findings approve that the proposed approach has aided in the utilization of a clean energy production system. Diesel generators dependency is reduced to 1.28%,

¹ In absence of a fixed exchange rate of the Lebanese pounds to dollar during the economic collapse Lebanon is facing today, the calculations performed in this work are associated to the official rate that remained pegged at 1515 L.B.P/\$

clean energy sources had a remarkable contribution of 20.66%, the overall system’s cost of energy is cut to 0.093\$/kWh, while a net annual savings of \$2,931,442 is achieved from the 1st year the proposed system is set into operation. Despite the insignificant virtual battery capacity that the e-scooter sharing system possess (0.576 kWh/scooter), this system showed a good contribution in supplying load by a share of 0.16% owing to the large quantity of use. Besides, the electrification of the AUB fleet holds an annual fuel cost savings of \$73,635 and a considerable portion of 1.22% in meeting demand during peak hours and grid outages.

Since MG optimal planning not only takes into account the energy needs to satisfy load but also aids in avoiding adverse effects on the environment by reducing CO₂ and other GHG emissions. Coupled with the desire to turn AUB campus into a clean sustainable one, AUB CO₂ emissions for the proposed new system have been investigated. This is depicted in Table 17. These findings point to a reduction of 2,767 tons of AUB CO₂ emissions in comparison to the current operating system. However, this number is slightly lower than what is expected due to the increasing grid’s electricity consumption to charge BSS, EVs, and e-scooters.

Emissions Source	Current AUB Carbon Emissions (in tons of CO₂/year)	Proposed System’s Carbon Emissions (in tons of CO₂/year)
Fuel Emissions from Transport Vehicles	185	39
Emissions from Grid’s Electricity Consumption	22,656	31,601
Emissions from diesel generators	12,079	513

Total Emissions	34,920	32,153
-----------------	--------	--------

6.3. Financial and Sensitivity Analysis

A detailed financial analysis over a 12-years is carried on in this section for the current operating system at AUB and the proposed one. This is followed by a sensitivity analysis to evaluate the performance of the proposed system if variations in the values of the proposed system parameters strike in the future.

6.3.1 Current Operating System Financial Analysis:

The current system is composed of diesel generators and grid as the main energy sources. This system is assessed by assuming that EDL tariff rates and diesel generators output energy remain constant while diesel and gasoline fuel prices experience a yearly increase of 1%. The MG performance under these conditions is depicted in Table 18. Accordingly, it can be noticed that the system’s cost of energy is expected to reach a value of 18.1 ¢/kWh in the 12th year.

Table 18: Performance evaluation of the current operating system over a 12 year period.

<i>Years</i>	1	<i>.....</i>	12
<i>AUB Load (KWh)</i>	46,543,950	<i>.....</i>	46,543,950
<i>EDL Energy (KWh)</i>	30,208,624	<i>.....</i>	30,208,624
<i>EDL total cost (\$)</i>	2,953,308	<i>.....</i>	2,953,308
<i>Diesel Gen Energy (KWh)</i>	16,335,326	<i>.....</i>	16,335,326
<i>DG total cost (\$)</i>	4,900,598	<i>.....</i>	5,467,442
<i>Total Cost (\$)</i>	7,853,906	<i>.....</i>	8,420,750
<i>Cost of Energy (\$/KWh)</i>	0.169	<i>.....</i>	0.181
<i>Cost of Fuel for Conventional Vehicles (\$)</i>	93,128	<i>.....</i>	103,900
<i>Total Cost (\$)</i>	7,947,034	<i>.....</i>	8,524,650

6.3.2 Proposed System Financial Analysis

To evaluate the economic advantages of the proposed (PV-BSS-DG-EVs-Scooters) system, the following assumptions have been considered in the proposed case analysis:

- Diesel and gasoline fuel prices are escalated by 1% per year.
- Loans associated to all system components are to be fully paid by AUB.

It is worth mentioning that the e-scooters reinvestment cycle is considered to be 3 years. This is due to the fact that the battery lifespan, in general, depends on its type and number of charging cycles. FITRIDER T2S can undergo more than 1000 charging cycles before its effectiveness gradually diminish and no longer functions at all. Hence, the lifespan of the e-scooter sharing project is assumed to be 3 years. Initially, the investment of the e-scooter sharing system considers the integration of 500 units. Whereas, its reinvestment at the 4th, 7th, and 10th years considers the purchase of 250 new e-scooters and the replacement of 250 batteries associated with 250 e-scooters from the previous investment cycle which are assumed to be in good physical conditions. The cost of each swappable battery is 170\$/unit.

The optimal operation of the MG must satisfy the previously outlined technical, economical, and environmental constraints and is conducted for a 12 years. Simulation results of the proposed system are summarized in Table 19. As detailed below the cost of energy resulting from the proposed system is lower than that of the current operating one by scoring a difference of 7.6 ¢/kWh in the first year. This value then rises smoothly over the years to reach a maximum of 0.1 \$/kWh at the 9th and 10th year and then falls sharply to its lowest value 0.072 \$/kWh during the last two years. Results also illustrate that the proposed MG optimal planning approach attained significant savings over the years to reach a maximum of around \$4.7 million on the 12th year. Diesel generator costs and dependency is reduced to a large extent in comparison to the existing scheme. The e-scooter's sharing service showed remarkable profits that cover

its annual loan payment and achieve an excess of \$325,381. However, this excess increases in the 4th year due to the reinvestment strategy discussed earlier.

This proposed system guarantees a positive cash flow in the 4th year from setting it into operation.

Table 19: Yearly financial and energy outcomes of the proposed system.

Years	1	2	3	4	5	6
<i>EDL Energy (KWh)</i>	42,134,462	42,043,063	41,948,937	41,817,315	41,727,683	41,631,722
<i>EDL total cost (\$)</i>	3,571,773	3,590,509	3,607,840	3,628,940	3,641,341	3,652,434
<i>Diesel Generators Energy (KWh)</i>	693,301	761,073	832,196	933,619	1,003,951	1,080,588
<i>Diesel Generators total cost (\$)</i>	207,990	230,605	254,677	288,573	313,415	340,713
<i>Reduction in Diesel Generator cost (%)</i>	96	95	95	94	94	93
<i>Battery Energy (KWh)</i>	5,971,324	5,752,542	5,539,537	5,259,902	5,081,181	4,902,315
<i>Battery Cost (\$)</i>	1,031,835	1,031,835	1,031,835	1,031,835	1,031,835	1,031,835
<i>PV Energy (KWh)</i>	4,441,521	4,441,521	4,441,521	4,441,521	4,441,52	4,441,521
<i>PV total cost (\$)</i>	292,886	292,886	292,886	292,886	292,886	292,886
<i>EVs Energy (KWh)</i>	656,987	656,987	656,987	656,987	656,987	656,987
<i>EVs total Cost (\$)</i>	216,996	216,996	216,996	216,996	216,996	216,996
<i>Conventional Vehicles Gasoline Cost (\$)</i>	19,493	19,688	19,885	20,084	20,285	20,488
<i>E-Scooters Energy (KWh)</i>	85,677	85,751	85,832	85,934	86,004	86,008
<i>E-Scooters Cost (\$)</i>	219,129	219,129	219,129	142,475	142,475	142,475
<i>E-Scooters Revenues (\$)</i>	544,511	544,511	544,511	544,511	544,511	544,511
<i>E-Scooters Total Cost (\$)</i>	(325,382)	(325,382)	(325,382)	(402,036)	(402,036)	(402,036)
<i>System Total Cost (\$)</i>	5,015,592	5,057,138	5,098,737	5,077,277	5,114,721	5,153,314
<i>Cost of Energy (\$/KWh)</i>	0.093	0.094	0.095	0.095	0.096	0.097
<i>Yearly Savings (\$)</i>	2,931,442	2,939,834	2,948,671	3,021,072	3,035,079	3,048,450
<i>Cash Flow (\$)</i>	(11,382,270)	(6,681,589)	(1,972,072)	2,305,768	7,025,039	11,757,680

Years	7	8	9	10	11	12
<i>EDL Energy (KWh)</i>	41,553,895	41,477,158	41,407,876	41,346,592	41,290,941	41,245,885
<i>EDL total cost (\$)</i>	3,660,096	3,666,980	3,672,287	3,676,132	3,679,064	3,681,085
<i>Diesel Generator Energy (KWh)</i>	1,143,601	1,206,166	1,263,196	1,314,155	1,360,770	1,398,726
<i>Diesel Generator Total Cost (\$)</i>	364,186	387,952	410,358	431,182	450,941	468,154
<i>Reduction in Diesel Generator Cost (%)</i>	93	93	92	92	92	91
<i>Battery Energy (KWh)</i>	4,765,163	4,633,904	4,520,504	4,424,919	4,341,281	4,275,566

<i>Battery Cost (\$)</i>	1,031,835	1,031,835	1,031,835	1,031,835	25,985	25,985
<i>PV Energy (KWh)</i>	4,441,521	4,441,521	4,441,521	4,441,521	4,441,521	4,441,521
<i>PV total cost (\$)</i>	292,886	292,886	292,886	292,886	21,144	21,144
<i>EVs Energy (KWh)</i>	656,987	656,987	656,987	656,987	656,987	656,987
<i>EVs total Cost (KWh)</i>	216,996	216,996	216,996	216,996	0.00	0.00
<i>Conventional Vehicles Gasoline Cost (\$)</i>	20,693	20,899	21,108	21,320	21,533	21,748
<i>E-Scooters Energy (KWh)</i>	86,032	86,106	86,106	86,106	86,106	86,106
<i>E-Scooters Cost (\$)</i>	142,475	142,475	142,475	142,475	142,475	142,475
<i>E-Scooters Revenues (\$)</i>	544,511	544,511	544,511	544,511	544,511	544,511
<i>E-Scooters Total Cost (\$)</i>	(402,036)	(402,036)	(402,036)	(402,036)	(402,036)	(402,036)
<i>System Total Cost (\$)</i>	5,184,655	5,215,512	5,243,434	5,268,314	3,796,630	3,816,079
<i>Cost of Energy (\$/KWh)</i>	0.098	0.099	0.100	0.100	0.072	0.073
<i>Yearly Savings (\$)</i>	3,069,594	3,091,747	3,117,364	3,146,559	4,672,858	4,708,571
<i>Cash Flow (\$)</i>	16,084,042	20,859,980	25,661,535	30,064,862	34,880,195	39,731,241

6.3.3. Sensitivity Analysis

The variation in the values of the financial parameters assumed in this study might cause infeasibility or economically expensive designs of the MG. Thus to mitigate this drawback, figures 15 and 16 represent two different possible economic cases. Figure 15 describes the impact of the loan's interest rate variations on the proposed system's yearly savings. It is apparent that this parameter plays a vital role in dropping the system's yearly savings as it increases. The system experiences a cut of an average of \$0.127, \$0.327, and \$0.468 million associated with 7%, 10%, and 12% interest rates, respectively in comparison to the base case interest rate of 5%. No effect of the interest rates variations in the 11th and 12th years because the loan is fully paid at the 10th year. In the last two years' savings strike and achieve a maximum value of \$4.7 million. The increase in the interest rates might also affect the payback period which increases from the 4th year to the 5th year when the interest rate hits 10% and 12%.

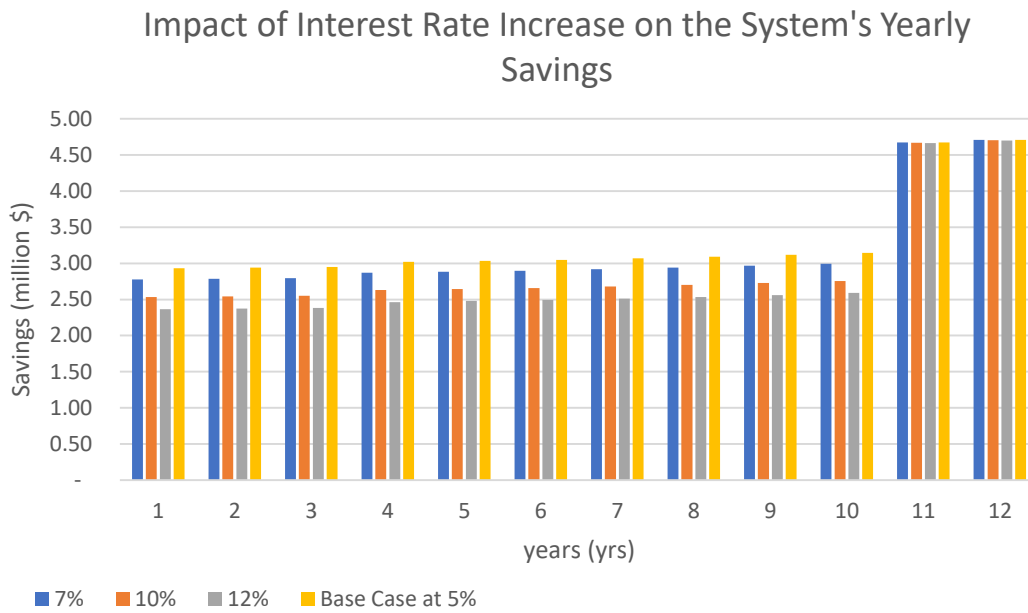


Figure 15: Impact of loan's interest rates increase on the system's yearly savings

Figure 16 illustrates the benefits of donations that might be afforded to support such green and clean initiatives. Two different scenarios were tested against the full loan payments. It can be interpreted from figure 19 that donations of 15% and 30% can increase the system's yearly savings by an average of \$0.24 and \$0.48 million, respectively. In the last two years' savings strike and achieve a maximum value of \$4.72 million. These donations can bring down the system's payback period to the 3rd year.

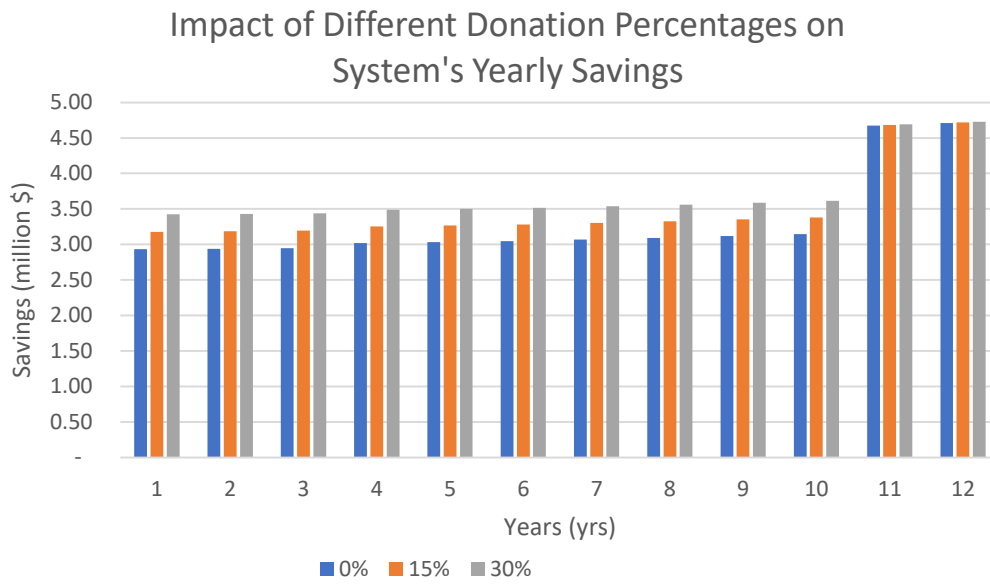


Figure 16: Impact of different donation percentages on the system's yearly savings.

CONCLUSION

This research aimed to redesign the power supply system of the American University of Beirut characterized by a scheduled grid's blackouts. The proposed system has been able to turn AUB campus into a green sustainable one, enhance campus energy security, reduce site emissions, decrease dependency on diesel generators to supply load during grid outages, and diminish power purchased at peak tariff hours.

Besides, this work has led us to determine the potential of introducing an e-scooter sharing system that will help AUB community to commute easily on campus. This has been achieved by analyzing the results of a conducted web-based questionnaire that targets the perceptions of respondents on various attributes of the sharing system. The majority of the respondents supported this service concept and expressed their willingness to use it in their future everyday life by stating their commuting patterns and rating its suggested fares.

These goals were achieved by implementing two main optimization stages. The first optimization level converges to the optimal BSS, PV and charge rate per kilometer by optimizing a rule-based EMS using PSO and FMINCON via Yalmip parser. The rule-based energy management algorithm aims to prioritize the utilization of clean resources and coordinate the power flow of the MG components. The second stage aims to optimally operate the MG under an optimal EMS which finds the optimal performance of such MG using convex optimization method.

The simulation findings reveal the proposed technique's superiority in minimizing the daily operational cost of the MG, contributing to better adoption of clean energy resources, and reducing diesel dependency during outages.

This research imposes several benefits and gains to the Lebanese community as it represents a model that can be implemented by all Lebanese people, public sector institutions, hospitals and universities to resolve the grid's blackout issues and reduce diesel dependency in meeting load demand. Moreover, the resulted findings and the adopted optimization approaches in this work when taught in energy-related courses can enhance student's knowledge in demonstrating the value of clean energy sources and EVs, their contribution to a more sustainable energy system, and the significant role they can play in supplying load demand during grid's outages in Lebanon. Due to the multiple benefits the proposed approach can achieve, further research can be conducted on enhancing the MG's EMS and optimization approaches under different operation conditions.

APPENDIX

The conducted survey conveys various perspectives associated with the integration of the e-scooters project at AUB campus as a mean of everyday commute. To reveal the attractiveness of such a project, Figure 17 describes how interested the respondents are in using an e-scooter service on campus to aid their commute. Most of them supported this concept and found it very appealing and regarded e-scooters as a must-have mode of commute. Those respondents accounted for 52% of the sample size. A feedback of 16% considered a neutral response. However, 8% of responders were not so interested in it and 4% were not excited at all and consider it a non-essential service.

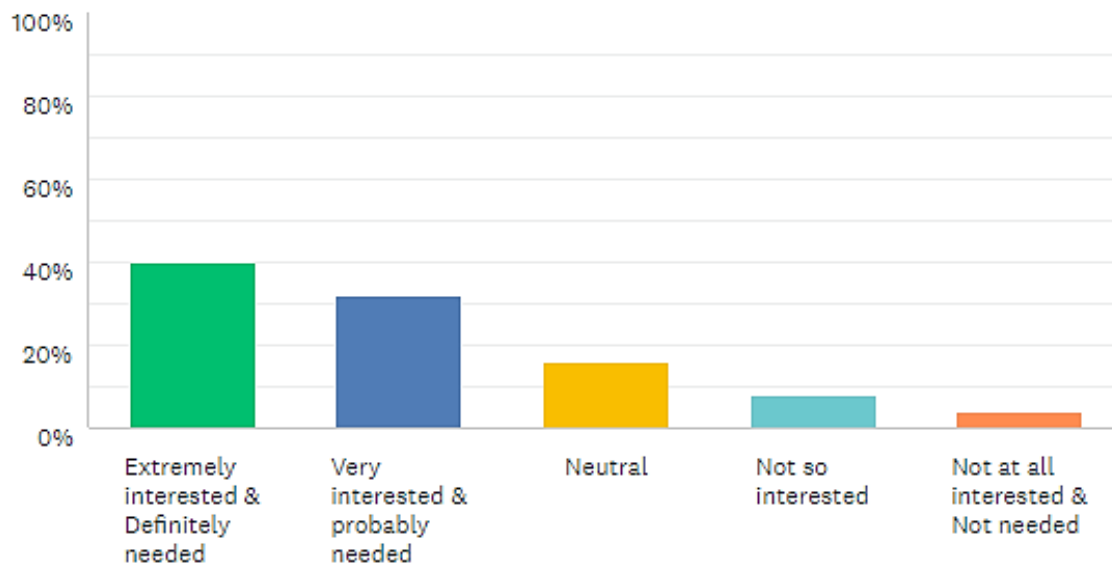
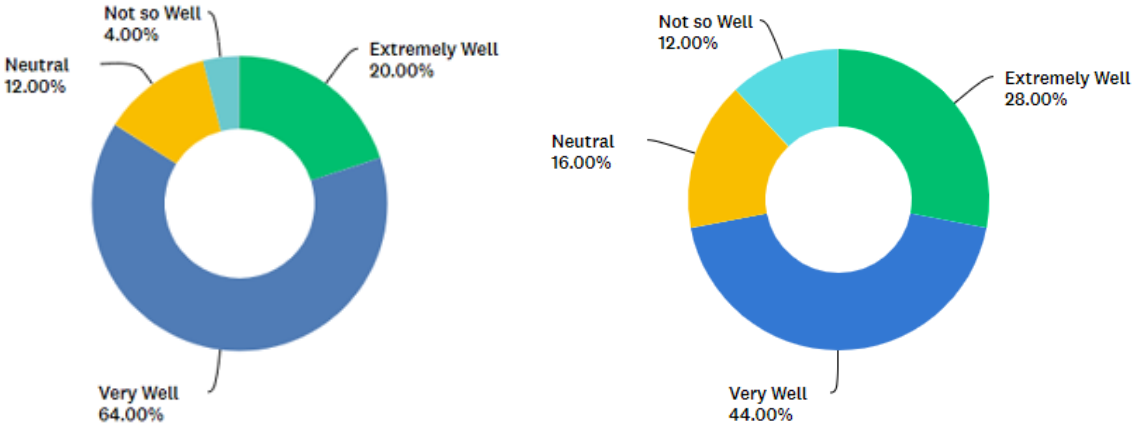


Figure 17: Respondents perspective on integrating an e-scooter commuting service on campus.

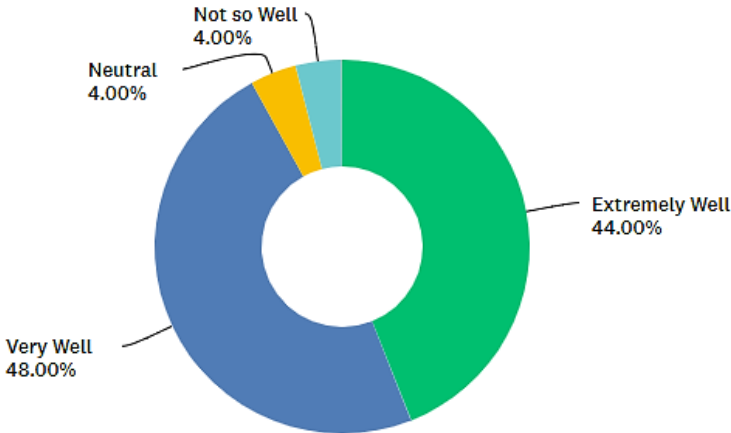
To investigate this system further, the survey included questions that aim to rate various service attributes in terms of network coverage, convenience, service time window, connectivity, accessibility, and safety measures. Figure 18 illustrates respondents' perceptions of these features. In general, these attributes significantly meet the respondents' expectations and are found to be very satisfying and fundamental aspects

of the service system. This can be interpreted from the respondent’s positive ratings (well/extremely well) that accounted for 84 % on safety measures, 72% on network coverage and accessibility, and 92% on service time window and convenience.



(a) Service safety measures

(b) Network coverage and accessibility



(c) Service time window and convenience

Figure 18: Respondent's perceptions on various e-scooter service attributes in terms of safety measures (scooter lanes and speed limit), network coverage (stations locations), accessibility (subscriptions and pay per use) and time window and convenience.

As a matter of fact, these findings indicate that there is a promising potential opportunity for integrating an e-scooter sharing system on AUB campus. Yet, a key barrier to the success of this project is the fare associated with each kilometer covered.

To evaluate this crucial element two questions were asked to the survey respondents. The first one aims to discover their expectations on the charge rate per kilometer to be imposed upon using the e-scooter service. The responses, in this case, span over a range that has a minimum of 0.33 \$/km and a maximum of 4\$/km. While the second question asks them to rank three price ranges. These ranges with their associated ratings are described in Figure 19. As can be noticed, the most rated range to be set as an appropriate fare for this service is 1.32\$/km – 1.65\$/km.

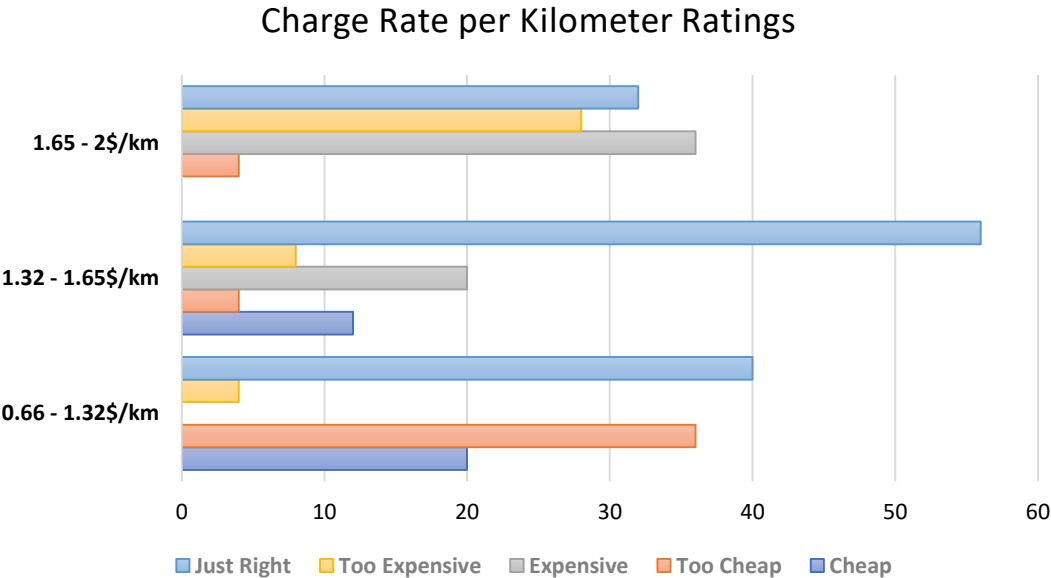


Figure 19: Ratings of different price ranges.

REFERENCES

- [1] V. S. Bhadoria, N. S. Pal, and V. Shrivastava, "A Review on Distributed Generation Definitions and DG Impacts on Distribution System," *Int. Conf. Adv. Comput. Commun. Technol.*, no. August 2014, pp. 1–7, 2013, doi: 10.13140/RG.2.1.4439.4328.
- [2] A. Hirsch, Y. Parag, and J. Guerrero, "Microgrids: A review of technologies, key drivers, and outstanding issues," *Renew. Sustain. Energy Rev.*, vol. 90, no. September 2017, pp. 402–411, 2018, doi: 10.1016/j.rser.2018.03.040.
- [3] J. Hu, T. Zhang, S. Du, and Y. Zhao, "An Overview on Analysis and Control of Micro-grid System," *Int. J. Control Autom.*, vol. 8, no. 6, pp. 65–76, 2015, doi: 10.14257/ijca.2015.8.6.08.
- [4] X. Zhou, T. Guo, and Y. Ma, "An overview on microgrid technology," *2015 IEEE Int. Conf. Mechatronics Autom. ICMA 2015*, pp. 76–81, 2015, doi: 10.1109/ICMA.2015.7237460.
- [5] B. S. Hartono, Budiyanto, and R. Setiabudy, "Review of microgrid technology," *2013 Int. Conf. Qual. Res. QiR 2013 - Conjunction with ICCS 2013 2nd Int. Conf. Civ. Sp.*, no. June, pp. 127–132, 2013, doi: 10.1109/QiR.2013.6632550.
- [6] E. De Din, C. Joglekar, G. Lipari, F. Ponci, and A. Monti, "An emergency energy management system for microgrid restoration after blackout," *2018 Int. Conf. Smart Energy Syst. Technol. SEST 2018 - Proc.*, pp. 1–6, 2018, doi: 10.1109/SEST.2018.8495669.
- [7] M. Alramlawi, A. Gabash, and P. Li, "Optimal operation strategy of a hybrid PV-battery system under grid scheduled blackouts," *Conf. Proc. - 2017 17th IEEE Int. Conf. Environ. Electr. Eng. 2017 1st IEEE Ind. Commer. Power Syst. Eur. IEEEIC / I CPS Eur. 2017*, 2017, doi: 10.1109/IEEEIC.2017.7977543.
- [8] K. M. Tan, V. K. Ramachandramurthy, and J. Y. Yong, "Integration of electric vehicles in smart grid: A review on vehicle to grid technologies and optimization techniques," *Renew. Sustain. Energy Rev.*, vol. 53, pp. 720–732, 2016, doi: 10.1016/j.rser.2015.09.012.
- [9] S. Bahramirad, W. Reder, and A. Khodaei, "Reliability-constrained optimal sizing of energy storage system in a microgrid," *IEEE Trans. Smart Grid*, vol. 3, no. 4, pp. 2056–2062, 2012, doi: 10.1109/TSG.2012.2217991.
- [10] X. Y. Wang, D. M. Vilathgamuwa, and S. S. Choi, "Determination of battery storage capacity in energy buffer for wind farm," *IEEE Trans. Energy Convers.*, vol. 23, no. 3, pp. 868–878, 2008, doi: 10.1109/TEC.2008.921556.
- [11] J. K. Kaldellis, D. Zafirakis, and E. Kondili, "Optimum sizing of photovoltaic-energy storage systems for autonomous small islands," *Int. J. Electr. Power Energy Syst.*, vol. 32, no. 1, pp. 24–36, 2010, doi: 10.1016/j.ijepes.2009.06.013.
- [12] N. A. Luu, Q. T. Tran, S. Bacha, and V. L. Nguyen, "Optimal sizing of a grid-connected microgrid," *Proc. IEEE Int. Conf. Ind. Technol.*, vol. 2015-June, no. June, pp. 2869–2874, 2015, doi: 10.1109/ICIT.2015.7125521.
- [13] E. L. Karfopoulos *et al.*, "Introducing electric vehicles in the microgrids concept," *2011 16th Int. Conf. Intell. Syst. Appl. to Power Syst. ISAP 2011*, 2011, doi: 10.1109/ISAP.2011.6082212.
- [14] D. Thomas, O. Deblecker, and C. S. Ioakimidis, "Optimal operation of an energy management system for a grid-connected smart building considering photovoltaics' uncertainty and stochastic electric vehicles' driving schedule,"

- Appl. Energy*, vol. 210, pp. 1188–1206, 2018, doi: 10.1016/j.apenergy.2017.07.035.
- [15] S. G. Yoon and S. G. Kang, “Economic microgrid planning algorithm with electric vehicle charging demands,” *Energies*, vol. 10, no. 10, 2017, doi: 10.3390/en10101487.
- [16] E. Mortaz and J. Valenzuela, “Microgrid energy scheduling using storage from electric vehicles,” *Electr. Power Syst. Res.*, vol. 143, pp. 554–562, 2017, doi: 10.1016/j.epsr.2016.10.062.
- [17] C. S. Ioakimidis, D. Thomas, P. Rycerski, and K. N. Genikomsakis, “Peak shaving and valley filling of power consumption profile in non-residential buildings using an electric vehicle parking lot,” *Energy*, vol. 148, pp. 148–158, 2018, doi: 10.1016/j.energy.2018.01.128.
- [18] Z. Wang and S. Wang, “Grid power peak shaving and valley filling using vehicle-to-grid systems,” *IEEE Trans. Power Deliv.*, vol. 28, no. 3, pp. 1822–1829, 2013, doi: 10.1109/TPWRD.2013.2264497.
- [19] M. Zhang and J. Chen, “The energy management and optimized operation of electric vehicles based on microgrid,” *IEEE Trans. Power Deliv.*, vol. 29, no. 3, pp. 1427–1435, 2014, doi: 10.1109/TPWRD.2014.2303492.
- [20] L. Zhou, F. Li, C. Gu, Z. Hu, and S. Le Blond, “Cost/benefit assessment of a smart distribution system with intelligent electric vehicle charging,” *IEEE Trans. Smart Grid*, vol. 5, no. 2, pp. 839–847, 2014, doi: 10.1109/TSG.2013.2282707.
- [21] C. T. Li, C. Ahn, H. Peng, and J. Sun, “Integration of plug-in electric vehicle charging and wind energy scheduling on electricity grid,” *2012 IEEE PES Innov. Smart Grid Technol. ISGT 2012*, pp. 1–7, 2012, doi: 10.1109/ISGT.2012.6175617.
- [22] K. Hyvönen, P. Repo, and M. Lammi, “Light Electric Vehicles: Substitution and Future Uses,” *Transp. Res. Procedia*, vol. 19, no. June, pp. 258–268, 2016, doi: 10.1016/j.trpro.2016.12.085.
- [23] R. R. Clewlow, “No Title The Micro-Mobility Revolution: The Introduction and Adoption of Electric 6 Scooters in the United States,” in *Transportation Research Board 98th Annual Meeting*, 2019, pp. 19–03991, [Online]. Available: <https://trid.trb.org/view/1572549>.
- [24] N. Zuniga-garcia, “Dockless Electric Scooters and Transit Use in an Urban / University Environment,” no. January, 2020.
- [25] R. Zhu, X. Zhang, D. Kondor, P. Santi, and C. Ratti, “Understanding spatio-temporal heterogeneity of bike-sharing and scooter-sharing mobility,” *Comput. Environ. Urban Syst.*, vol. 81, no. March, p. 101483, 2020, doi: 10.1016/j.compenvurbsys.2020.101483.
- [26] G. Mckenzie, “Spatiotemporal comparative analysis of scooter-share and bike-share usage patterns in Washington , D . C .,” no. June 2019, 2020, doi: 10.1016/j.jtrangeo.2019.05.007.
- [27] S. Zhou, Y. Ni, and X. Zhang, “Effects of dockless bike on modal shift in metro commuting: A pilot study in shanghai,” in *Proceedings of the Transportation Research Board 97th Annual Meeting*, 2018, pp. 18–04973.
- [28] D. J. Reck, S. Guidon, H. He, and K. W. Axhausen, “Explaining shared micromobility usage, competition and mode choice by modelling empirical data from Zurich, Switzerland,” 2020.
- [29] A. A. Campbell, C. R. Cherry, M. S. Ryerson, and X. Yang, “Factors influencing the choice of shared bicycles and shared electric bikes in Beijing,” *Transp. Res.*

- Part C*, vol. 67, pp. 399–414, 2016, doi: 10.1016/j.trc.2016.03.004.
- [30] S. Munira and I. N. Sener, “Use of Direct-Demand Modeling in Estimating Nonmotorized Activity: A Meta-analysis,” 2017. [Online]. Available: https://www.vtti.vt.edu/utc/safe-d/wp-content/uploads/2018/04/UTC-Safe-D_Direct-Demand-Model-for-PedBike_TTI-Report_12Oct17_Final.pdf.
- [31] D. Buck, R. Buehler, P. Happ, B. Rawls, P. Chung, and N. Borecki, “Are Bikeshare Users Different from Regular Cyclists? A First Look at Short-Term Users, Annual Members, and Area Cyclists in the Washington, D.C., Region,” *Transp. Res. Rec.*, no. 2387, pp. 112–119, 2013, doi: 10.3141/2387-13.
- [32] J. Degele *et al.*, “Identifying E-Scooter Sharing Customer Segments Using Clustering,” in *2018 IEEE International Conference on Engineering, Technology and Innovation (ICE/ITMC)*, Jun. 2018, pp. 1–8, doi: 10.1109/ICE.2018.8436288.
- [33] M. Lee, J. Y. J. Chow, G. Yoon, and B. Y. He, “Forecasting e-scooter competition with direct and access trips by mode and distance in New York City,” *arXiv*, 2019.
- [34] W. El-Assi, M. Salah Mahmoud, and K. Nurul Habib, “Effects of built environment and weather on bike sharing demand: a station level analysis of commercial bike sharing in Toronto,” *Transportation (Amst.)*, vol. 44, no. 3, pp. 589–613, 2017, doi: 10.1007/s11116-015-9669-z.
- [35] J. Bachand-Marleau, B. Lee, and A. El-Geneidy, “Better understanding of factors influencing likelihood of using shared bicycle systems and frequency of use,” *Transp. Res. Rec.*, no. 2314, pp. 66–71, 2012, doi: 10.3141/2314-09.
- [36] D. A. Hensher, P. Stopher, and P. Bullock, “Service quality - developing a service quality index in the provision of commercial bus contracts,” *Transp. Res. Part A Policy Pract.*, vol. 37, no. 6, pp. 499–517, 2003, doi: 10.1016/S0965-8564(02)00075-7.
- [37] J. M. del Castillo and F. G. Benitez, “Determining a public transport satisfaction index from user surveys,” *Transp. A Transp. Sci.*, vol. 9, no. 8, pp. 713–741, 2013, doi: 10.1080/18128602.2011.654139.
- [38] R. Imam, “Measuring Public Transport Satisfaction from User Surveys,” *Int. J. Bus. Manag.*, vol. 9, no. 6, 2014, doi: 10.5539/ijbm.v9n6p106.
- [39] R. F. Abenoza, O. Cats, and Y. O. Susilo, “Travel satisfaction with public transport: Determinants, user classes, regional disparities and their evolution,” *Transp. Res. Part A Policy Pract.*, vol. 95, no. May 2020, pp. 64–84, 2017, doi: 10.1016/j.tra.2016.11.011.
- [40] M. H. Almannaa, F. A. Alshahaf, H. I. Ashqar, M. Elhenawy, M. Masoud, and A. Rakotonirainy, “Perception analysis of E-scooter riders and non-riders in Riyadh, Saudi Arabia: Survey outputs,” *Sustain.*, vol. 13, no. 2, pp. 1–22, 2021, doi: 10.3390/su13020863.
- [41] N. Hatziaargyriou, “Microgrids: Architectures and Control,” *Microgrids Archit. Control*, pp. 1–317, 2013, doi: 10.1002/9781118720677.
- [42] M. F. Zia, E. Elbouchikhi, and M. Benbouzid, “Microgrids energy management systems: A critical review on methods, solutions, and prospects,” *Appl. Energy*, vol. 222, no. May, pp. 1033–1055, 2018, doi: 10.1016/j.apenergy.2018.04.103.
- [43] C. Corchero and M. Cruz-zambrano, “Optimal Energy Management for a Residential Microgrid Including a Vehicle-to-Grid System,” vol. 5, no. 4, pp. 2163–2172, 2014.
- [44] S. Chalise, J. Sternhagen, T. M. Hansen, and R. Tonkoski, “Energy management of remote microgrids considering battery lifetime,” *Electr. J.*, vol. 29, no. 6, pp. 1–

- 10, 2016, doi: 10.1016/j.tej.2016.07.003.
- [45] L. U. U. N. An, "Optimal energy management for grid connected microgrid by using Dynamic programming method," no. 1, 2015.
- [46] H. Kanchev, B. F. S. Member, and V. Lazarov, "Unit commitment by dynamic programming for microgrid operational planning optimization and emission reduction," no. September, pp. 8–10, 2011.
- [47] M. Jevtic and D. Klimenta, "Energy and operation management of a microgrid using particle swarm optimization," no. June, 2015, doi: 10.1080/0305215X.2015.1057135.
- [48] L. Wang and C. Singh, "PSO-Based Multi-Criteria Optimum Design of A Grid-Connected Hybrid Power System With Multiple Renewable Sources of Energy," no. Sis, pp. 250–257, 2007.
- [49] K. Rahbar, J. Xu, and R. Zhang, "Real-time energy storage management for renewable integration in microgrid: An off-line optimization approach," *IEEE Trans. Smart Grid*, vol. 6, no. 1, pp. 124–134, 2015, doi: 10.1109/TSG.2014.2359004.
- [50] A. Chiş, J. Rajasekharan, J. Lundén, and V. Koivunen, "Demand response for renewable energy integration and load balancing in smart grid communities," *Eur. Signal Process. Conf.*, vol. 2016-Novem, pp. 1423–1427, 2016, doi: 10.1109/EUSIPCO.2016.7760483.
- [51] A. L. Motto, Y. Sun, and A. Chakraborty, "On global solution to a class of smart building-grid energy management models," *Proc. IEEE Conf. Decis. Control*, pp. 5580–5585, 2012, doi: 10.1109/CDC.2012.6426139.
- [52] M. Zolfaghari, N. Ghaffarzadeh, and A. J. Ardakani, "Optimal sizing of battery energy storage systems in off-grid micro grids using convex optimization," *J. Energy Storage*, vol. 23, no. February, pp. 44–56, 2019, doi: 10.1016/j.est.2019.02.027.
- [53] C. Tang, C. Liang, and Y. Hu, "A reliable quadratic programming algorithm for convex economic dispatch with renewable power uncertainty," *2018 8th Int. Conf. Power Energy Syst. ICPEs 2018*, pp. 40–43, 2019, doi: 10.1109/ICPEsYS.2018.8626913.
- [54] F. Fardoun, O. Ibrahim, R. Younes, and H. Louahlia-Gualous, "Electricity of Lebanon: Problems and recommendations," *Energy Procedia*, vol. 19, no. May, pp. 310–320, 2012, doi: 10.1016/j.egypro.2012.05.211.
- [55] S. LechtenbÄ¶hmer and S. Samadi, "The Power Sector," *Decarbonization Eur. Union*, 2015, doi: 10.1057/9781137406835.0009.
- [56] IRENA, *Renewable Energy Outlook: Lebanon*. 2020.
- [57] H. Amaar and M. Khatri, "The appropriate technique for modeling of solar photovoltaic module," no. December, 2020, doi: 10.1729/Journal.25159.
- [58] R. Chedid and A. Sawwas, "Optimal placement and sizing of photovoltaics and battery storage in distribution networks," *Energy Storage*, vol. 1, no. 4, pp. 1–12, 2019, doi: 10.1002/est.2.46.
- [59] "LG LG365Q1C-A5: High Efficiency LG NeON® R Module Cells: 6 x 10 Module efficiency: 21.1% Connector Type: MC4 | LG USA Business." <https://www.lg.com/us/business/solar-panels/lg-LG365Q1C-A5> (accessed Mar. 18, 2021).
- [60] "Module Efficiency Mean | Solar Energy Experts | Infinite Energy." <https://www.infiniteenergy.com.au/module-efficiency-mean/> (accessed Mar. 18,

- 2021).
- [61] A. S. Aziz, M. F. N. Tajuddin, M. R. Adzman, M. A. M. Ramli, and S. Mekhilef, "Energy management and optimization of a PV/diesel/battery hybrid energy system using a combined dispatch strategy," *Sustain.*, vol. 11, no. 3, 2019, doi: 10.3390/su11030683.
 - [62] R. Chedid, A. Sawwas, and D. Fares, "Optimal design of a university campus micro-grid operating under unreliable grid considering PV and battery storage," *Energy*, vol. 200, p. 117510, 2020, doi: 10.1016/j.energy.2020.117510.
 - [63] M. Azaza and F. Wallin, "Multi objective particle swarm optimization of hybrid micro-grid system : A case study in Sweden," *Energy*, vol. 123, pp. 108–118, 2017, doi: 10.1016/j.energy.2017.01.149.
 - [64] "BMW i4 price and specifications - EV Database." <https://ev-database.org/car/1252/BMW-i4> (accessed Apr. 19, 2021).
 - [65] "2021 Chevy Bolt EV: Affordable Electric Car | Chevrolet." <https://www.chevrolet.com/electric/bolt-ev> (accessed Apr. 19, 2021).
 - [66] "Lightning Electric Ford Transit Cargo Van | Lightning eMotors." <https://lightningemotors.com/lightningelectric-ford-transit-cargo/> (accessed Apr. 19, 2021).
 - [67] "MITSUBISHI FUSO TRUCK & BUS CORPORATION." https://pscfmjefdmcommon.blob.core.windows.net/fusoassets/2019/09/eCanter_Brochure_ENG_2019.pdf (accessed Apr. 19, 2021).
 - [68] "KIA e-Niro Electric Car | KIA Motors UK." <https://www.kia.com/uk/new-cars/e-niro/> (accessed Apr. 19, 2021).
 - [69] "Mercedes eSprinter electric van: price and specifications | DrivingElectric." <https://www.drivingelectric.com/mercedes-benz/sprinter> (accessed Apr. 19, 2021).
 - [70] "Nissan launches electric pickup truck with 250-mile range and nutty price through JV in China - Electrek." <https://electrek.co/2019/07/16/nissan-electric-pickup-truck-dongfeng-rich-6-ev/> (accessed Apr. 20, 2021).
 - [71] "PEUGEOT e-208 50 kWh Active 136 Auto - NewElectric (av UK mix) - CO2 0 g/km." [https://www.nextgreencar.com/view-car/73551/peugeot-e-208-50-kwh-active-136-auto-electric-\(av-uk-mix\)/](https://www.nextgreencar.com/view-car/73551/peugeot-e-208-50-kwh-active-136-auto-electric-(av-uk-mix)/) (accessed Apr. 20, 2021).
 - [72] "New Peugeot e-Partner electric van to go on sale in late 2021 | DrivingElectric." <https://www.drivingelectric.com/peugeot/partner> (accessed Apr. 20, 2021).
 - [73] "R1T - Rivian." <https://rivian.com/r1t> (accessed Apr. 20, 2021).
 - [74] "Renault Kangoo Maxi ZE 33 price and specifications - EV Database." <https://ev-database.org/car/1101/Renault-Kangoo-Maxi-ZE-33> (accessed Apr. 20, 2021).
 - [75] "2016 Tesla Model S 70 Specifications - The Car Guide." <https://www.guideautoweb.com/en/makes/tesla/model-s/2016/specifications/70/> (accessed Apr. 20, 2021).
 - [76] "Factory New Engergy Lithium Battery 8m 20 Seat Electric Bus - Buy Battery Power Electric Bus,16-20 Seat Mini Bus,Price Of New Electric Bus Product on Alibaba.com." https://www.alibaba.com/product-detail/factory-new-engergy-lithium-battery-8m_62404663950.html?spm=a2700.7724857.normalList.50.74ca7eccifT25f (accessed Apr. 20, 2021).
 - [77] "China Factory Best Price 15 Seats Pure Electric Passenger Van Mini Bus - Buy Mini Passenger Van, Van For Rent, Electric Van Product on Alibaba.com."

- https://www.alibaba.com/product-detail/China-factory-best-price-15-seats_62372923835.html?spm=a2700.7724857.normalList.12.374c6a5aarbEDm (accessed Apr. 20, 2021).
- [78] “china fitrider scooter factory.” <https://www.fitriderscooter.com/> (accessed Apr. 20, 2021).
- [79] “Hangzhou Fitcoo Technology Co.,Ltd.” <http://www.fitcoo.com/> (accessed Apr. 20, 2021).
- [80] J. Fong, P. Mcdermott, and M. Lucchi, “Micro-Mobility , E-Scooters and Implications for Higher Education,” no. May, pp. 1–21, 2019, [Online]. Available: <https://upcea.edu/micro-mobility-e-scooters-and-implications-for-higher-education/>.
- [81] “Building a Scooter Sharing App Like Lime, Nextbike, and Mobike | Mobindustry.” <https://www.mobindustry.net/building-a-scooter-sharing-app-like-lime-nextbike-and-mobike/> (accessed Mar. 28, 2021).
- [82] V. Meyrand, G. B. Tabet, and O. Kassamani, “Lebanon Municipality of Beirut Sustainable energy action plan (SEAP),” 2012, [Online]. Available: www.ces-med.eu.
- [83] M. O. Okwu and L. K. Tartibu, “Particle Swarm Optimisation,” *Stud. Comput. Intell.*, vol. 927, pp. 5–13, 2021, doi: 10.1007/978-3-030-61111-8_2.
- [84] S. Ebbesen, P. Kiwitez, and L. Guzzella, “A generic particle swarm optimization Matlab function,” *Proc. Am. Control Conf.*, no. November, pp. 1519–1524, 2012, doi: 10.1109/acc.2012.6314697.
- [85] D. G. Y. Rahmat-Samii and J. Robinson, “Particle swarm optimization (PSO): a novel paradigm for antenna designs,” *Radio Sci. Bull.*, vol. 305, no. 305, pp. 14–22, 2003.
- [86] J. Löfberg, “YALMIP: A toolbox for modeling and optimization in MATLAB,” *Proc. IEEE Int. Symp. Comput. Control Syst. Des.*, pp. 284–289, 2004, doi: 10.1109/cacsd.2004.1393890.
- [87] “Constrained Nonlinear Optimization Algorithms - MATLAB & Simulink.” <https://www.mathworks.com/help/optim/ug/constrained-nonlinear-optimization-algorithms.html> (accessed Apr. 10, 2021).
- [88] J. Agnarsson, M. Sunde, and I. Ermilova, “Parallel Optimization in Matlab,” no. January, pp. 1–47, 2013.
- [89] M. C. Grant and S. P. Boyd, “The CVX Users ’ Guide, Release 2.0 (beta),” 2013.

